Clim Dyn
DOI 10.1007/s00382-009-0543-6

Land surface coupling in regional climate simulations of the West African monsoon

Allison L. Steiner · Jeremy S. Pal · Sara A. Rauscher · Jason L. Bell · Noah S. Diffenbaugh · Aaron Boone · Lisa C. Sloan · Filippo Giorgi

Received: 15 May 2008 / Accepted: 16 February 2009
© Springer-Verlag 2009

Abstract Coupling of the Community Land Model (CLM3) to the ICTP Regional Climate Model (RegCM3) substantially improves the simulation of mean climate over West Africa relative to an older version of RegCM3 coupled to the Biosphere Atmosphere Transfer Scheme (BATS). Two 10-year simulations (1992–2001) show that the seasonal timing and magnitude of mean monsoon precipitation more closely match observations when the new land surface scheme is implemented. Specifically, RegCM3–CLM3 improves the timing of the monsoon advance and retreat across the Guinean Coast, and reduces a positive precipitation bias in the Sahel and Northern Africa. As a result, simulated temperatures are higher, thereby reducing the negative temperature bias found in the Guinean Coast and Sahel in RegCM3–BATS. In the RegCM3–BATS simulation, warmer temperatures in northern latitudes and wetter soils near the coast create excessively strong temperature and moist static energy gradients, which shifts the African Easterly Jet further north than observed. In the RegCM3–CLM3 simulation, the migration and position of the African Easterly Jet more closely match reanalysis winds. This improvement is triggered by drier soil conditions in the RegCM3–CLM3 simulation and an increase in evapotranspiration per unit precipitation. These results indicate that atmosphere–land surface coupling has the ability to impact regional-scale circulation and precipitation in regions exhibiting strong hydroclimatic gradients.

Keywords African monsoon · Land surface modeling · Soil moisture · Land surface–atmosphere coupling · RegCM3 · Regional climate modeling

A. L. Steiner (✉)
Department of Atmospheric, Oceanic and Space Sciences, University of Michigan, Ann Arbor, MI 48109-2143, USA
e-mail: alsteiner@umich.edu

J. S. Pal
Department of Civil Engineering and Environmental Science, Loyola Marymount University, Los Angeles, CA 90045-2659, USA

S. A. Rauscher · F. Giorgi
Earth System Physics – Weather and Climate Group, Abdus Salam International Centre for Theoretical Physics, 34014 Trieste, Italy

J. L. Bell · L. C. Sloan
Department of Earth and Planetary Sciences, University of California, Santa Cruz, CA 95064, USA

N. S. Diffenbaugh
Purdue Climate Change Research Center and Department of Earth and Atmospheric Sciences, Purdue University, West Lafayette, IN 47907-2051, USA

A. Boone
CNRS/GAME, CNRM Météo-France, Toulouse, France

1 Introduction

The land surface represents the lower atmospheric boundary condition for approximately 30% of the Earth's surface. The transfer of energy, mass and momentum between the biosphere and the atmosphere occurs at this interface, and the coupling between these two systems is known to impact local, regional and global climate. Regions where soil moisture anomalies cause large changes in regional circulation and climate have been termed "land-atmosphere hotspots" (Koster et al. 2004). These hotspots are often found in transition zones between wet and dry regimes. The seasonal monsoon in West Africa causes a strong gradient

Published online: 10 March 2009

between wet and dry regions, providing a trigger for the close coupling between the land and atmosphere. As a result, the timing and magnitude of the monsoon play a key role in the land-atmosphere feedbacks.

There are several mechanisms that allow soil moisture to impact land-atmosphere interactions. First, soil moisture can affect the precipitation recycling ratio (β), which is defined as the ratio of precipitation derived from the local evapotranspiration (ET) to the total moisture source (ET and moisture advected into a region (IN)):

$$\beta = \frac{\mathrm{ET}}{\mathrm{ET} + \mathrm{IN}} \tag{1}$$

The value of β indicates the "strength" of the coupling between the land surface and the atmosphere. For example, high values of β indicate that the majority of precipitation is due to local evapotranspiration and is recycled, whereas low β values suggest that the precipitation is derived from the moisture advection from outside the local region (Schär et al. 1999). Second, increased soil moisture can increase the efficiency of precipitation processes (Betts and Ball 1995; Betts et al. 1996). These two effects establish a positive feedback loop between soil moisture and precipitation. These soil moisture feedbacks are apparent in models (e.g., Schär et al. 1999) as well as observations (e.g., Koster et al. 2003) and can occur across a range of time-scales. For instance, soil moisture can influence the position of storm systems (Pal and Eltahir 2003; Taylor et al. 2005), as well as rainfall in future seasons (Pal and Eltahir 2001). Because of this soil moisture "memory" in the climate system (Vinnikov et al. 1996), accurate simulation of soil moisture processes is crucial for short-term precipitation forecasts, seasonal-scale predictions, and long-term climate projections.

Many factors can influence the formation, duration, and movement of the monsoon, including sea surface temperatures (SSTs) in the Atlantic, Indian, and Pacific Ocean basins (e.g., Janicot et al. 2001; Rowell 2001; Vizy and Cook 2001; Giannini et al. 2003; Messager et al. 2004; Paeth and Friederichs 2004; Joly et al. 2007), current and antecedent soil moisture conditions (Philippon and Fontaine 2002; Fontaine et al. 2002, 2007; Douville et al. 2007), inflow air mass characteristics (Chou and Neelin 2003), and vegetation feedbacks (Charney et al. 1977; Zheng and Eltahir 1998; Wang and Eltahir 2000; Abiodun et al. 2007). The feedback cycles between the land surface and the atmosphere in West Africa are described and diagnosed in detail in Philippon and Fontaine (2002), who highlight two main features that increase the efficiency of precipitation processes in the region. The first feature, the Bowen ratio effect, suggests that wetter soils cool and add more moisture to the near-surface atmospheric layers, effectively decreasing the Bowen ratio. This increases the moist entropy flux and the amount of convective available potential energy in the relatively shallow boundary layer (Schär et al. 1999; Pal and Eltahir 2001). The resulting vertical thermodynamic profile tends to become unstable, increasing the frequency and magnitude of convective rainfall events (Pal and Eltahir 2001). Lower temperatures cause a decrease in outgoing longwave radiation, while a moister atmosphere causes an increase in incoming longwave radiation, leading to an overall increase in net longwave radiation. The second feature, the albedo effect, is caused by wetter soils that are darker in color and allow more solar radiation to be absorbed at the surface. Both the Bowen ratio effect and the albedo effect lead to an increase in the total net surface radiation, which then increases the heat flux (sensible and latent) to the boundary layer. These increases in heat flux act to increase the moist static energy (MSE), defined as:

$$\mathrm{MSE} = gZ + c_pT + Lq \tag{2}$$

where g is the gravitational acceleration, Z is geopotential height, c_p is the specific heat capacity at constant pressure, L is the latent heat of vaporization, and q is the specific humidity. MSE can account for the transformation of sensible and latent heat fluxes from the lower troposphere into geopotential energy in the upper troposphere, and its meridional gradients can drive the monsoon circulation (Emanuel 1995). During the West African monsoon, an increase in heat flux caused by wetter soils can then lead to an increase in MSE in the boundary layer. Additionally, lower temperatures cause a decrease in boundary layer height, further increasing the MSE per unit depth of the boundary layer (Pal and Eltahir 2001). Depending on the magnitude and spatial pattern of MSE, the MSE meridional gradients can influence the timing of the monsoon penetration into the African continent, the occurrence of deep convection, and the magnitude of precipitation (Philippon and Fontaine 2002).

These land surface and atmospheric changes in temperature and MSE can also impact the large-scale circulation. For instance, meridional gradients of temperature and MSE affect the formation and development of the African Easterly Jet (AEJ), a midtropospheric jet located at approximately 600 hPa. This jet occurs over western Africa in the boreal summertime and migrates in a north–south direction with the monsoon circulation (e.g., Parker et al. 2005). The position and strength of the AEJ can influence the large-scale circulation in the region (Cook 1999). The AEJ forms as a result of a positive meridional surface temperature gradient over western Africa, with higher surface temperatures over the Sahara and cooler, moister air near the coast; this gradient reverses in the mid-troposphere near the vertical position of the AEJ (Burpee 1972; Cook 1999; Thorncroft and Blackburn 1999). Near

the surface, warmer temperatures over the Sahara create the Saharan Heat Low (SHL) and cyclonic circulation in the lower troposphere. Higher in the atmosphere, the descending branch of the Hadley cell creates subsidence aloft, causing the Saharan High to occur at approximately 600 hPa. Outflow from the Saharan high is deflected to the right due to the Coriolis force, creating the AEJ. The jet is partly maintained by an ageostrophic thermally direct circulation, where dry convection from the SHL induces a diabatic meridional circulation that induces a negative temperature gradient aloft (Thorncroft and Blackburn 1999). These dynamical mechanisms lead to the strong coupling between the land surface and atmosphere over western Africa, indicating that small perturbations in the land surface conditions can propagate vertically in the atmosphere and impact the regional atmospheric circulation.

This complex timing, spatial pattern and magnitude of the monsoon precipitation have traditionally been difficult for global and regional climate models to replicate (e.g., Cook and Vizy 2006; Meehl et al. 2006; Sijikumar et al. 2006), although some regional models have successfully simulated the monsoon precipitation in select years (Gallée et al. 2004; Messager et al. 2004). Previous RegCM3–BATS simulations of the African monsoon employing the convection scheme of Grell et al. (1994) capture the overall advance and retreat of the African monsoon, but overestimate the magnitude of the precipitation along the Guinean Coast and slightly underestimate precipitation in the Sahel (Afiesimama et al. 2006; Konaré et al. 2008). However, the magnitude of precipitation is reduced when the radiative effects of dust are included (Konaré et al. 2008). In addition, sensitivity experiments have shown that the location and intensity of the simulated monsoon band depends on the RegCM convection scheme (Pal et al. 2007; Abiodun et al. 2008).

In this study, we investigate the impact of different land surface parameterizations (LSPs) on the climate of the West Africa land-atmosphere hotspot, as simulated by a regional climate model. In fact, past studies have noted the importance of the LSP in this region (Diedhiou and Mahfouf 1996; Sijikumar et al. 2006). Here, we upgrade the land surface package of the regional climate model RegCM3 (Pal et al. 2007) from the Biosphere-Atmosphere Transfer Scheme (BATS; Dickinson et al. 1993) to the more advanced Community Land Model (CLM3; Oleson et al. 2004). In this paper, we compare the two LSP experiments in terms of the simulation of the West African monsoon and the dynamical mechanisms underlying its evolution. Specifically, we evaluate how the change in LSP affects the mean simulation of precipitation (Sect. 3), how the changes in the LSP affect soil moisture and the surface energy and water budgets (Sect. 4), and how these changes in surface properties alter to the atmosphere via MSE and the general circulation of the region (Sect. 5).

2 Methods

2.1 Description of RegCM3 and experiment design

The Regional Climate Model version 3 (RegCM3) is an evolution of the model originally developed at the National Center for Atmospheric Research (NCAR) and currently maintained at the International Centre for Theoretical Physics (ICTP) (Pal et al. 2007). RegCM3 is a grid-point limited area model with a hydrostatic dynamical core (similar to the NCAR/PSU MM5; Grell et al. 1994), a full radiation package (CCM3; Kiehl et al. 1996) allowing for the effects of greenhouse gases and atmospheric aerosols, a non-local planetary boundary layer scheme (Holtslag et al. 1990), and multiple convection schemes (e.g., Emanuel 1991; Grell 1993). It has been tested in a variety of domains throughout the world (c.f., Giorgi et al. 2006 and references therein), and has been shown to simulate climate in various mid-latitude and tropical regions with reasonable accuracy (Pal et al. 2007). Further details about RegCM3 can be found in Pal et al. (2007) and references therein.

We select a model domain spanning a range of climatic zones from the tropics to midlatitudes. Our initial focus of analysis is western Africa, a region that is expected to have strong land-atmosphere coupling. The full domain encompasses equatorial and northern Africa along with continental Europe, ranging from approximately 5°S to 55°N, and from 20°W to 40°E (Fig. 1). The horizontal resolution is 60 km, with 18 atmospheric layers from the surface to 100 hPa. Three-dimensional atmospheric boundary conditions are provided by the ECMWF 40-year Reanalysis (ERA-40; Uppala et al. 2005) at 2.5° spatial resolution and 6-h temporal resolution. Weekly SSTs are obtained from the NOAA optimum interpolation (OI) SST analysis (Version 2; Reynolds et al. 2002) and are linearly interpolated to daily values in the model. Land cover data is derived from 1 km Global Land Cover Classification data (GLCC) version 2 data provided by the U.S. Geological Survey (USGS) Earth Resources Observation Center (Loveland et al. 2000), where the GLCC International Geosphere-Biosphere Programme (IGBP) land cover categories are matched to BATS land cover categories. Our experiments use the MIT-Emanuel scheme (Emanuel 1991) to simulate convective precipitation, which is the same scheme used by Pal et al. (2007), and the SUBEX scheme to simulate large-scale precipitation (Pal et al. 2000). We note that RegCM3 has the option of different convective schemes, which are known to produce different results over this region (Afiesimama et al. 2006; Abiodun

et al. 2008; Konaré et al. 2008). We perform two 10-year simulations from 1992 to 2001: one with RegCM3–BATS and the second with RegCM3–CLM3.

In order to evaluate the progression of the monsoon in our simulations, we focus on three western Africa regions: the Guinean Coast (4–10°N, 10W–10°E), the Sahel (10–20°N, 10W–30°E) and Northern Africa (20–30°N, 10W–30°E) (regions shown in Fig. 1). As the monsoon progresses northward over land (moving from the equator to 15°N), the magnitude of precipitation increases with time successively in each of these regions until the monsoon retreats in autumn.

2.2 Land surface models: BATS and CLM3

The current LSP in the standard version of the RegCM3—the Biosphere-Atmosphere Transfer Scheme (BATS; Dickinson et al. 1993)—has been a component of the RegCM system since the 1990s (Giorgi et al. 1993). BATS is a "second-generation" land surface model, which uses a force-restore method to calculate soil temperature, has three soil layers for interactive soil moisture calculations, one bulk snow layer, a one-layer vegetation scheme and a simple description of surface runoff. As part of the community effort to develop RegCM3, we coupled the NCAR version of the Community Land Model (CLM3) to the RegCM3 atmosphere. The CLM3 is a state-of-the-science LSP developed and supported by NCAR (Oleson et al. 2004). CLM3 represents a "third-generation" land surface model, meaning that it includes a physical representation of the coupling between the water, energy and carbon cycles (Sellers et al. 1997). A detailed description of the differences between BATS and an earlier version of CLM, CLM0, is presented in Dai et al. (2003) and Steiner et al. (2005).

Earlier coupled versions of RegCM and CLM0 (Steiner et al. 2005) indicate that the updated land surface scheme improves the agreement between simulated climate and ground-based observations, primarily because of an improved representation of root zone soil moisture and its impact on the surface energy and water budgets. The CLM3 uses a series of biogeophysical parameterizations to describe the exchange of energy, momentum, water and carbon between the land surface and the atmosphere.

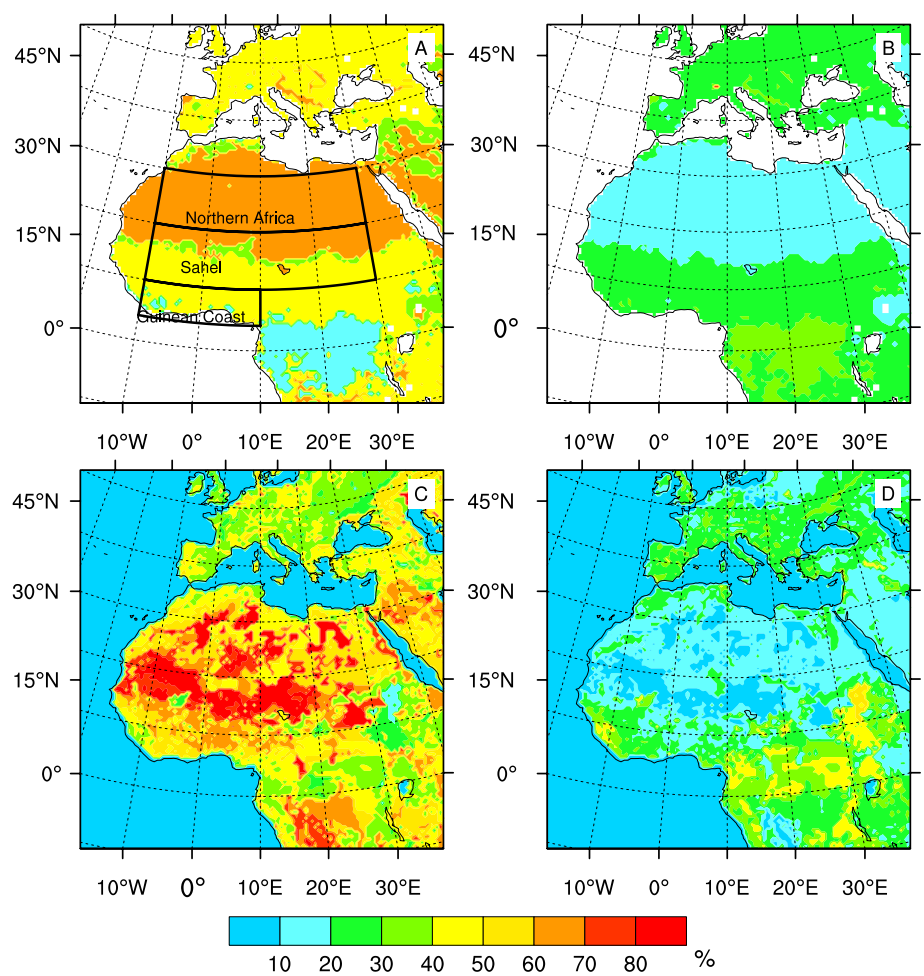

Fig. 1 Soil texture for (**a**) BATS % sand, (**b**) BATS % clay, (**c**) CLM3% sand, and (**d**) CLM3% clay. BATS soil texture data from land cover type and the FAO Soil Map of the World (FAO/UNESCO 1974) and CLM3 soil texture data from the Global Soil Data Task (2000). The three regions of analysis (Guinean Coast, Sahel and Northern Africa) are outlined in (**a**)

Within each atmospheric model grid cell, CLM3 treats land surface heterogeneity using the "mosaic" method (Koster and Suarez 1992), which divides each cell into a subgrid hierarchy composed of land units (representing glacier, wetland, lake, urban, and vegetated land cover), and a second and third hierarchy for vegetated landunits, including different snow/soil columns (for different vegetation fractions), and plant functional types (PFTs) (Oleson et al. 2004). Biogeophysical processes are simulated for each landunit, column and PFT separately, and then averaged for return to the atmospheric model. CLM3 biogeophysical properties add additional detail, including a coupled photosynthesis-stomatal conductance model, in-canopy radiation schemes, revised snow parameterizations and hydrology, and a river runoff scheme (Oleson et al. 2004).

2.3 Soil properties and soil moisture initialization

One of the primary differences between the two land surface models is the description and physical parameterization of the soil water column. BATS describes the soil column with three layers: a surface layer (the top 10 cm), a root zone layer (the top 1–2 m of soil depending upon the land cover type), and the total soil column (3–5 m and specified to 3 m in this study). CLM3 explicitly solves a ten-layer soil model. Because BATS has a simpler description of the soil column, we convert the 10 CLM3 layers into each of the three BATS soil layers in order to make a direct comparison between the two models. The BATS surface layer corresponds to the first three layers of CLM3 soil layers. In CLM3, the root zone includes the first eight to nine layers of the CLM3 soil column, depending on the land cover type. In the following analysis, we focus on the surface and root zones, as these two portions of the column will exhibit the strongest influence on the surface evaporation fluxes. In general, the surface soil moisture affects ground evaporation, while the root zone soil moisture has a greater influence on the transpiration by vegetation. Therefore, the greatest impact of the deep reservoir of soil moisture will be found in regions with high tree cover, such as the Guinean Coast.

The treatment of the land surface hydrology in the two schemes has numerous differences. For instance, hydraulic properties such as porosity, hydraulic conductivity and soil matric potential in CLM3 are based on the soil texture (percent sand and percent clay), which has greater detail than the limited soil texture description in BATS (based on 12 specified soil texture categories, see further discussion below). CLM3 calculates a groundwater table depth to determine saturated and unsaturated zones in the soil, which in turn influences subsurface runoff (Oleson et al. 2004). In contrast, runoff in BATS is a simple function of precipitation rate and soil water content relative to saturation. The CLM3 hydrology has the ability to account for both liquid water and ice in the soil, while BATS only accounts for liquid water.

In addition to revised model physics, different soil texture input datasets are used in the two models (Fig. 1). In the standard RegCM version, BATS assigns one of twelve soil texture categories based on the FAO Soil Map of the World (Wilson 1984; FAO/UNESCO 1974) and land cover type. CLM3 uses sand and clay contents from the 5-minute resolution IGBP soil dataset (Global Soil Data Task 2000) to develop a depth-variant soil texture dataset (Bonan et al. 2002). As a result, the CLM3 soil texture dataset has a higher resolution of data in both the horizontal and vertical dimensions. The soils in CLM3 have a higher sand content of up to 20% than those in BATS in the Sahel and Northern Africa (Fig. 1). Clay content in CLM3 (20–50%) is slightly higher than in BATS (20–40%) in sub-Saharan Africa and slightly lower in the Sahara (up to 10%).

Additionally, the soil moisture initialization strategies vary between the two land models. BATS initializes soil moisture by prescribing the soil water content relative to saturation as a function of land cover type (Giorgi and Bates 1989). This leads to an initial total soil water column of about 700–1000 mm H_2O over the majority of the land domain, with a lower initial soil water column of 100–300 mm H_2O over the Sahara. In contrast, CLM3 is initialized in our experiments with its default setting of 0.3 $mm^3\ mm^{-3}$, or 30% of the soil column for approximately 1000 mm H_2O over all land regions. As a result, the CLM3 simulation is initially wetter than the RegCM3–BATS simulation, particularly in the Sahara region. We conduct 2 years of additional model simulation (1990–1991) prior to the full 10-year simulation (1992–2001) to allow the soil moisture to equilibrate, and these two spinup years are not included in the subsequent analysis. Depending on the geographic location and precipitation regime, soil moisture initialization has varying importance (Koster and Suarez 2003) and can take months to years to reach equilibrium (Cosgrove et al. 2003; de Goncalves et al. 2006). In our ten year simulations, continued drying was noted in the Sahel and Northern African regions by about 20 mm H_2O over the ten year period (about 10% and 18% reductions, respectively), particularly in the CLM3 simulation. However, no substantial effects in the simulated precipitation and temperature were noted when comparing the first two years of the simulation (1992–1993) and last two years of the simulation (2000–2001) with observations (results not shown). Therefore, the 2-year spinup appears to be sufficient for most regions of the domain to reach an equilibrium of soil moisture–atmosphere interactions.

2.4 Observations

Simulated precipitation and temperature are evaluated using gridded monthly datasets derived from observations, including gridded station data from the Climate Research Unit at the University of East Anglia (CRU) at 0.5° latitude/longitude resolution (Mitchell et al. 2004). Because station data are sparse over some areas of our domain, we also employ the Climate Prediction Center Merged Analysis of Precipitation (CMAP) gridded data set at 2.5° latitude/longitude resolution (Xie and Arkin 1997), which is a blended product of global satellite and gauge data.

Due to the lack of soil moisture and surface flux observations over western Africa during our simulation time period, we compare the average root zone seasonal soil moisture cycle and the surface latent and sensible heat fluxes with data from the AMMA Land Surface Model Intercomparison Project (ALMIP). The ALMIP study is a multi-model comparison of eleven land surface models forced by a combination of NWP and satellite-based observations including TRMM 3B24 V6 precipitation (Boone et al., The AMMA Land Surface Model Intercomparison Project (ALMIP), submitted to the *Bulletin of the American Meteorological Society*). The ALMIP regional domain ranges from 20°W to 30°E and from 5°S to 20°N for the years 2004–2007 (Boone and deRosnay 2007), comparable to our Guinean Coast and Sahel regions. The ALMIP model output is therefore akin to a reanalysis product and provides the best available soil moisture and surface flux data on a broad spatial scale over the region (Dirmeyer et al. 2006). Despite the different years of simulation (1992–2001 for the RegCM simulations and 2004–2007 in ALMIP), we compare our RegCM3 results with the ALMIP model results for representative wet and dry years.

3 Impact of LSP on precipitation

3.1 Timing and magnitude of mean precipitation

The West African monsoon onset typically occurs in early spring (March–April), with the largest precipitation amounts along the Guinean Coast. In the boreal summer

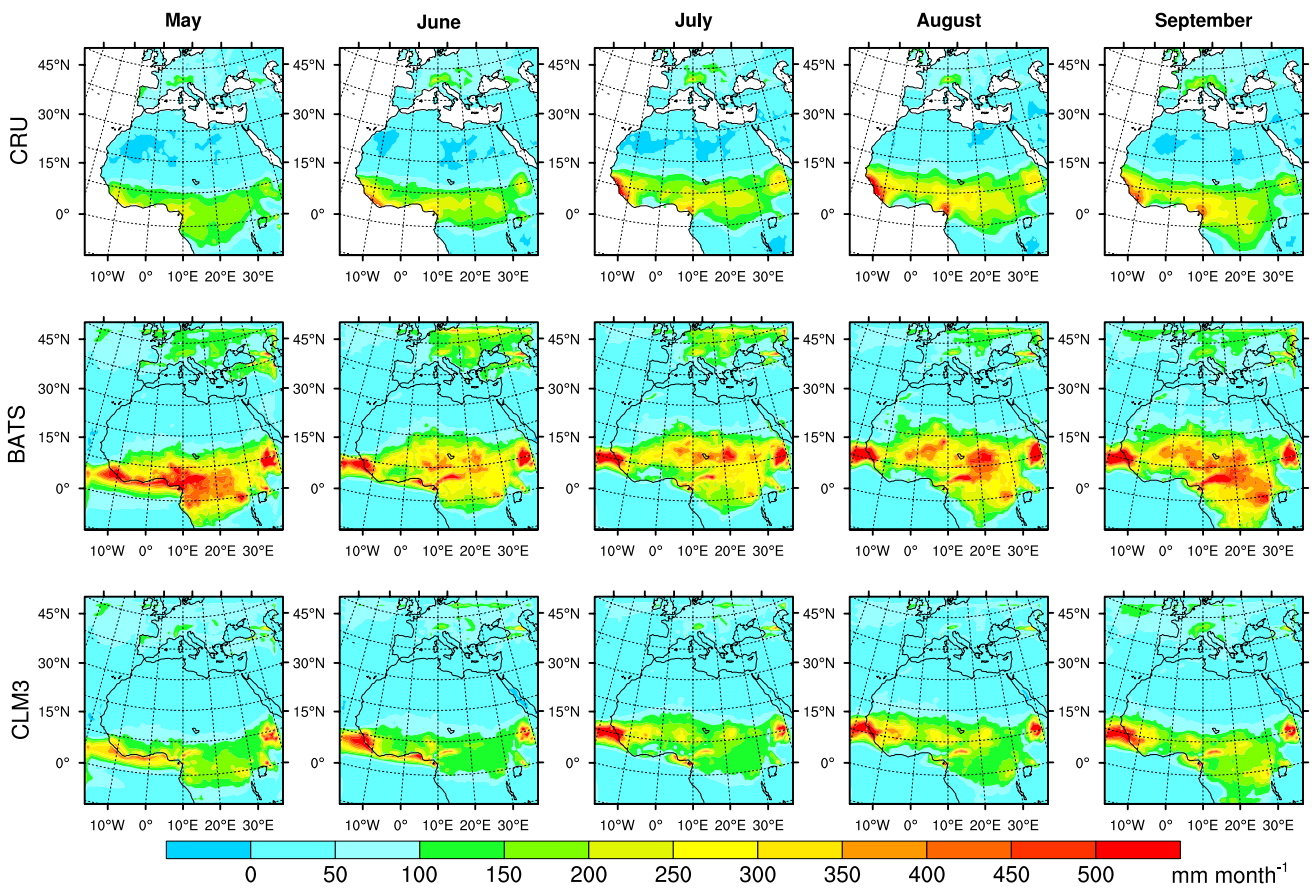

Fig. 2 Average monthly (May–September) precipitation (mm month^{-1}) over the 10 year simulation time period (1992–2001) for CRU observations (*top panel*), BATS model simulations (*middle panel*) and CLM3 model simulations (*bottom panel*)

months (June–July–August (JJA)), the monsoon migrates northward and inland, with maximum precipitation values of 300–500 mm month^{-1} in August (Fig. 2). In fall, the monsoon retreats south, passing over the Guinean Coast in September–October (SO). In the following discussion, biases are presented with respect to the CRU data only. Figure 3 shows that the CMAP observations are very similar to the CRU data over the three regions.

Comparison of the RegCM3–BATS simulation with CRU observations shows the model simulates too much precipitation in the monsoon band and produces an excessively northward migration of the monsoon rain band during May through September (Figs. 2, 3 and Table 1). During the monsoon advance in May, biases of up to 200 mm month^{-1} (110%) occur in the Guinean Coast region, and up to 100 mm month^{-1} in the Sahel region (Fig. 3). As the monsoon progresses northward in June, RegCM3–BATS exhibits a negative precipitation bias in the Guinean Coast region. This is due to an excessive northward displacement of the monsoon front in the RegCM3–BATS simulation. The premature advance yields a spurious bimodal seasonal distribution of precipitation over the Guinean Coast, with a first peak occurring when the monsoon advances over the region in March–April–May (MAM) and a second peak occurring when the monsoon retreats in October and November. This bimodal distribution is not evident in the CRU or CMAP observations (Fig. 3). This accelerated advance also causes a positive

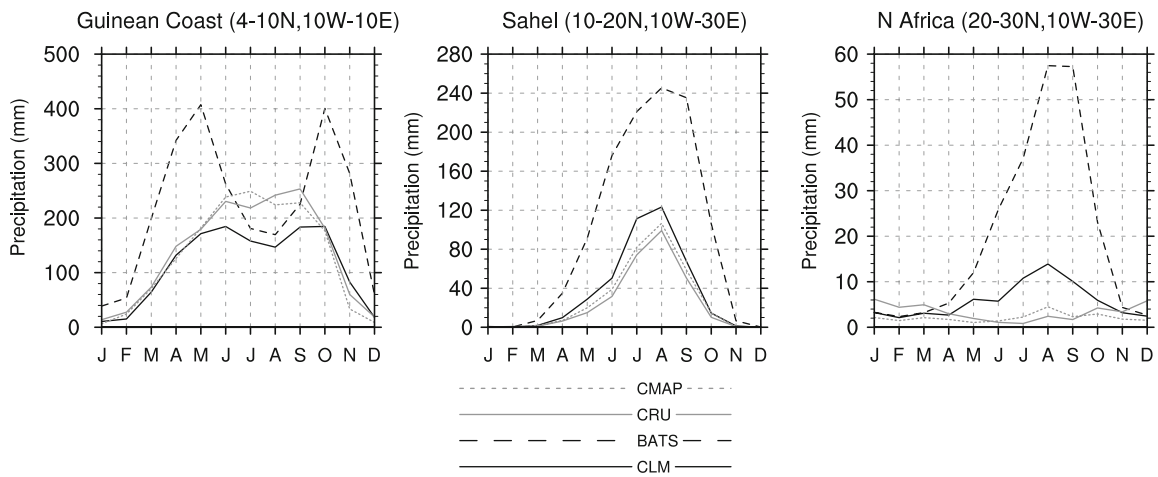

Fig. 3 Average seasonal precipitation (mm month^{-1}) for the three West African regions (Guinean Coast, Sahel and Northern Africa) over the 10 year simulation period (1992–2001) for CRU (Mitchell et al. 2004; *gray solid line*) and CMAP (Xie and Arkin 1997; *gray dotted line*), RegCM–CLM3 (*black solid line*) and RegCM3–BATS simulations (*black dashed line*)

Table 1 Seasonal observed temperature and precipitation data (CRU; Mitchell et al. 2004) and RegCM3–BATS and RegCM3–CLM3 modeled biases (model-observations). Precipitation biases are shown in reference to the CRU dataset only

	Temperature (°C)				Precipitation (mm H_2O month^{-1})			
	DJF	MAM	JJA	SON	DJF	MAM	JJA	SON
Guinean Coast								
CRU	27.1	28.1	25.4	26.0	22.4	136.0	229.4	161.9
Bias BATS	−1.3	−1.8	−1.7	−1.6	23.8	180.1	−25.2	140.7
Bias CLM	0.1	−0.7	−1.8	−1.3	−9.5	−13.4	−66.4	−11.6
Sahel								
CRU	21.9	30.0	31.2	28.6	0.6	8.0	67.5	19.9
Bias BATS	−1.5	−0.9	−2.9	−2.4	−0.04	36.4	146.6	96.2
Bias CLM	−0.9	−1.0	−1.9	−0.8	−0.4	5.5	27.5	8.0
Northern Africa								
CRU	14.3	23.1	31.8	24.5	5.4	3.8	1.5	3.0
Bias BATS	−1.2	1.3	0.7	−1.4	−2.6	3.1	38.7	25.2
Bias CLM	−1.9	−0.4	−0.5	−1.3	−2.7	0.2	8.6	3.4

bias of 150 mm month^{-1} in the Sahel region and 50 mm month^{-1} in northern Africa. (We note that the low number of observing stations over this particular region creates high uncertainty in the observed regional precipitation.) The RegCM3–BATS simulation indicates a slow retreat of the monsoon that stretches into October, leading to a bias of 110 mm month^{-1} in the Sahel region and over 220 mm month^{-1} (120%) in the Guinean Coast region. It should be noted that the precipitation overestimate in this simulation is at least partially related to the use of the Emanuel scheme, which tends to produce higher precipitation amounts than the Grell scheme over tropical regions (Pal et al. 2007).

The change to the CLM3 land surface scheme has a strong effect on the simulated monsoon precipitation patterns. In the RegCM3–CLM3 experiment (Figs. 2, 3), the magnitude and timing of precipitation are substantially improved. During the advance of the monsoon in April and May, biases in the Guinean Coast region are slightly negative (on the order of 10–20 mm month^{-1}, or 10%; Table 1) and biases in the Sahel region are positive (approximately 10 mm month^{-1}, or 50%). In the Guinean Coast region, the bimodal distribution of precipitation predicted by the RegCM3–BATS simulation is much less pronounced in the RegCM3–CLM3. While the RegCM3–CLM3 simulation underestimates precipitation slightly (bias of 50–80 mm month^{-1}, or about 30%) in June and July, the magnitude and timing of the spring and fall precipitation improve. In the Sahel region, RegCM3–CLM3 has a slight positive bias during most of the monsoon season (Table 1), but the magnitude of excess precipitation is reduced compared to RegCM3–BATS. In the Northern Africa region, RegCM3–CLM3 substantially lowers the bias to a seasonal maximum of 10 mm month^{-1} compared to the observations. Overall, the monsoon timing improves in the RegCM3–CLM3 compared to the RegCM3–BATS.

3.2 Simulation of interannual precipitation variability

In addition to the simulation of mean precipitation, RegCM3–CLM3 also improves the simulation of interannual precipitation variability. Using the 1992–2001 time period as a baseline, both the CRU and CMAP observations show large interannual variations in precipitation (Fig. 4). For example, in the Sahel region, observed precipitation indicates that certain years are drier (1992–1993, 2000–2001) or wetter (1998–1999) than the 10-year climatological average. While these wet and dry anomalies do not occur simultaneously in all three regions, the years 1994 and 1999 are consistently wetter in two out of three regions, while years 1992, 2000 and 2001 are consistently drier in all three regions. In general, the RegCM3–CLM3 produces this variability with higher fidelity than RegCM-BATS. Correlation coefficients with CRU and CMAP observations for RegCM3–CLM3 are typically twice those of RegCM-BATS, with similar coefficients for the model simulations when using either the CMAP or CRU dataset (Fig. 4).

Overall, these results show that RegCM3–CLM3 considerably improves the simulation of the monsoon precipitation over West Africa relative to RegCM3–BATS for the present model configuration. In the following sections, we analyze the mechanism underlying the effects of the LSP on the model's climatology, by investigating the impact on surface properties such as soil moisture (Sect. 4.1.1), the surface water and energy budgets (Sects. 4.1.2 and 4.1.3), and the influence of these changes on the atmosphere via the effect of moist static energy on the atmospheric circulation (Sect. 5).

4 Impact of LSP change on surface properties

4.1 Surface water balance

4.1.1 Soil moisture

Large differences in simulated precipitation are likely to cause substantial differences in soil moisture. As described in Sect. 2.3, the soil description and moisture representations are quite different between the two LSPs. The surface zone soil moisture is higher in RegCM3–BATS than in RegCM3–CLM3 over the full annual cycle in most regions, with the exception of the dry season (December–January–February (DJF)) in the Sahel and the Northern Africa regions (Fig. 5). In the Guinean Coast region, the seasonal pattern of soil moisture in the RegCM3–BATS simulation follows that of precipitation, with an increase in MAM as the monsoon advances, a decrease in JJA as the monsoon moves further north, and a second peak in SO as the monsoon retreats. The RegCM3–CLM3 simulation exhibits a similar cycle, although the bimodal seasonal distribution in soil moisture is suppressed following the precipitation cycle. In the Guinean Coast region, RegCM3–CLM3 surface soil moisture is approximately 40–50% lower than in RegCM3–BATS over the full seasonal cycle. Similar patterns occur in the Sahel region, where the RegCM3–CLM3 has a much smaller seasonal amplitude than the RegCM3–BATS and lower soil moisture of up to 60% during the peak monsoon season (JJA). In the Northern Africa region, RegCM3–CLM3 has a damped seasonal soil moisture cycle relative to RegCM3–BATS, which shows a strong peak in the boreal summer (JJA) that is approximately 70% greater than in the RegCM3–CLM3 surface soil moisture. Due to the lack of a strong seasonal cycle in precipitation over Northern Africa in the RegCM3–CLM3 simulation, soil moisture varies little seasonally.

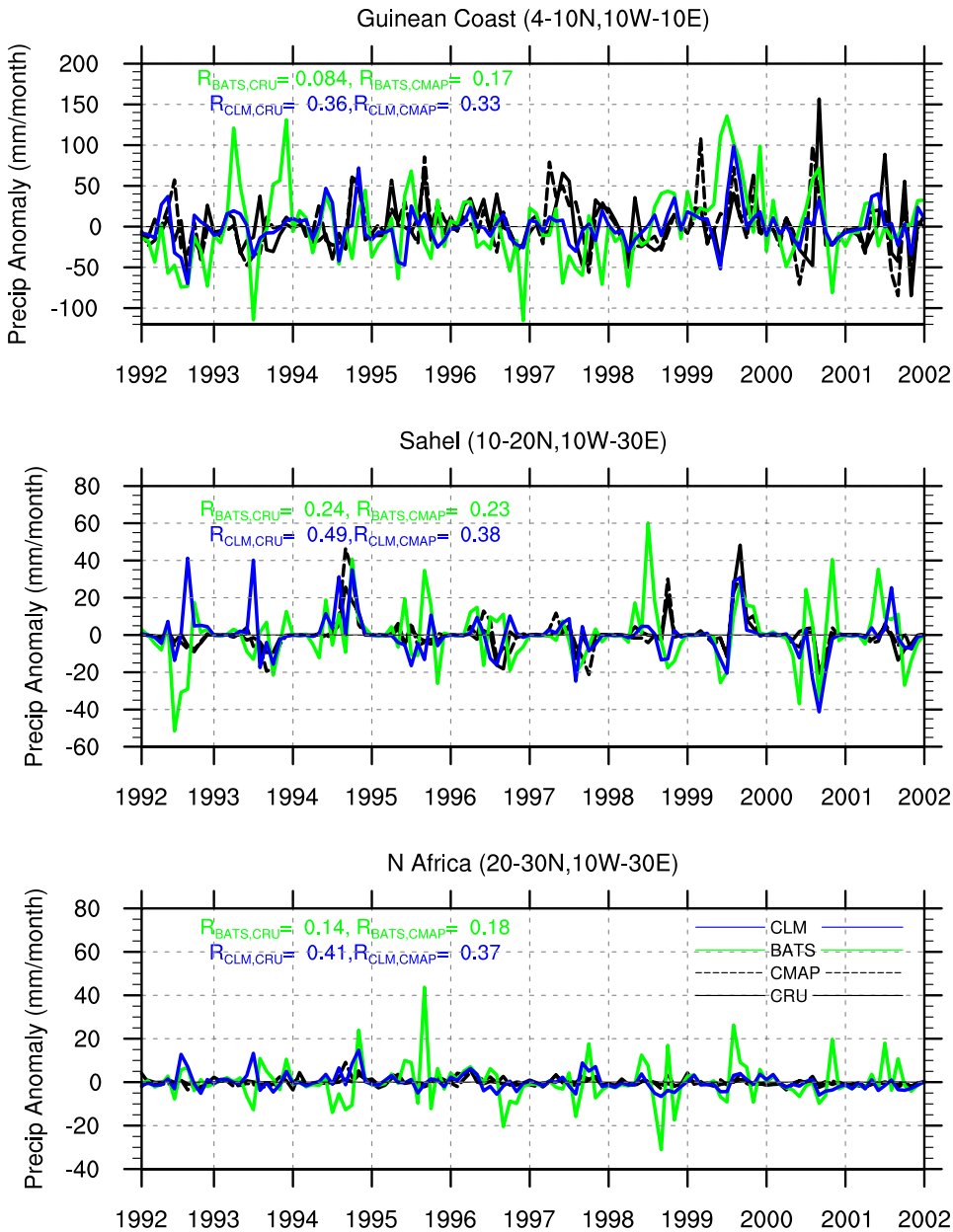

Fig. 4 Interannual precipitation variability (mm month^{-1}) for the RegCM3–CLM3 (*blue*) and RegCM3–BATS (*green*) simulations with CRU (*black solid*) and CMAP (*black dashed*) observations. Anomalies are calculated based on the 1992–2001 mean for RegCM3–BATS, RegCM3–CLM3, CRU observations, and CMAP observations. Correlation coefficients for each simulation with each precipitation dataset are listed for each region

As with surface soil moisture, the root zone soil moisture is consistently greater in RegCM3–BATS than in RegCM3–CLM3 over the full seasonal cycle. This difference is clear in the comparison of a representative dry year of our simulation time period (1992) with a representative wet year (1999) (Fig. 6). In the Guinean Coast region, the root zone soil moisture in RegCM3–BATS is 15–20% higher than in RegCM3–CLM3, with a damped bimodal seasonal peak associated with the advance and retreat of the monsoon. Root zone soil moisture differences between RegCM3–BATS and RegCM3–CLM3 reach up to 30% in the Sahel (Fig. 6) and up to 15% in northern Africa (not shown).

Figure 6 shows the ALMIP multi-model mean root zone soil moisture from this experiment, along with the inter-model standard deviation for a representative dry year (2005) and representative wet year (2007), compared with the RegCM3 dry year (1992) and wet year (1999). Note that the large spread of data across the models is partly due to the different definitions of root zone soil moisture between models. The ALMIP TRMM precipitation forcing is also shown, and indicates a good agreement with the RegCM3–CLM3 simulated precipitation. In the Guinean Coast region, the RegCM3–CLM3 simulation shows less seasonal amplitude than the ALMIP multi-model mean root zone soil moisture in both dry and wet years. In the

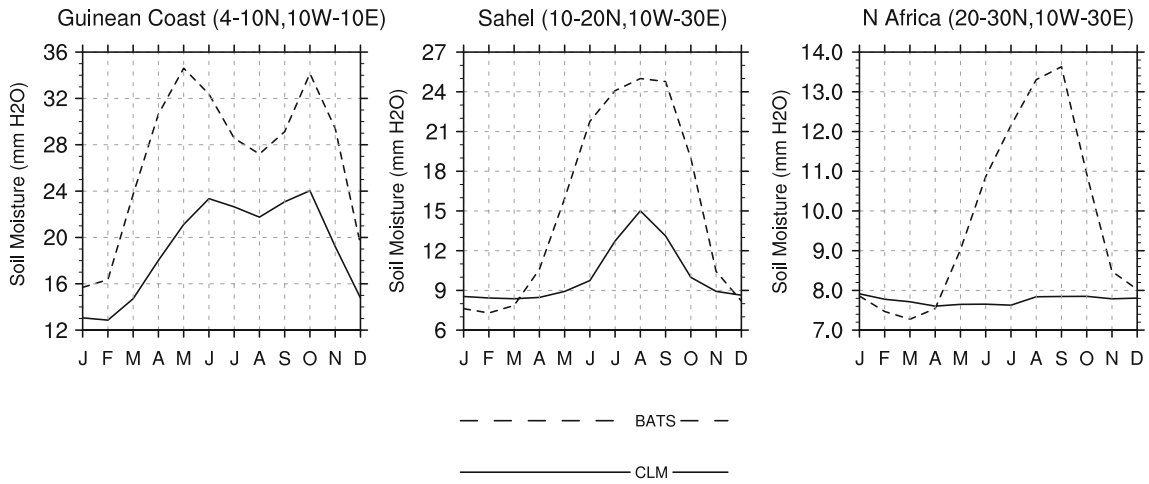

Fig. 5 Average seasonal surface soil moisture (first 10 cm from the surface) (mm H_2O) for the three West African regions over the 10 year simulation period (1992–2001) for the RegCM3–CLM3 simulations (*black solid*) and RegCM3–BATS simulations (*black dashed*)

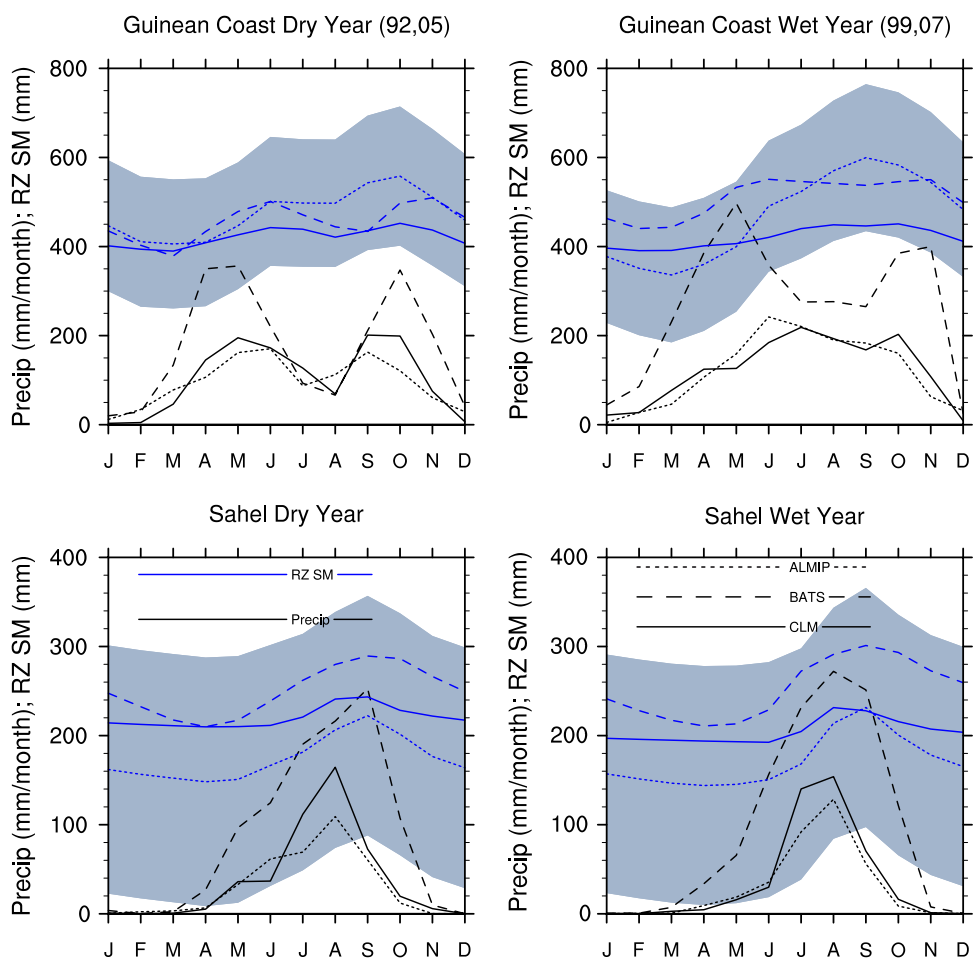

Fig. 6 Average seasonal precipitation (*black*) and root zone soil moisture (*blue*; first 1–2 m from the surface) (mm H_2O) for the three West African regions over the 10 year simulation period (1992–2001) for the RegCM3–CLM3 simulations (*solid line*) and RegCM3–BATS simulations (*dashed line*). The TRMM-derived precipitation forcing for the AMMA Land Model Intercomparison Project (ALMIP) experiments (*black dashed line*) is shown to compare the driving meteorology for the ALMIP land surface simulations. Root zone soil moisture for the ALMIP multi-model mean (2004–2006) is shown in the *dotted blue line*, with ± one standard deviation (*shaded blue*)

Sahel region, both RegCM3–BATS and RegCM3–CLM3 have more root zone soil moisture than the ALMIP model mean, but RegCM3–CLM3 is more similar to the ALMIP data in both dry and wet years. This comparison of RegCM3 root zone soil moisture with the ALMIP data suggests that the seasonal cycle of soil moisture in RegCM3 may be damped compared to other LSPs.

As noted in Sect. 2.3, the use of varying soil boundary conditions may have an impact on the soil moisture and precipitation results. In order to evaluate the impact of soil

texture on soil moisture and precipitation, we conducted sensitivity tests in which the CLM3 soil texture dataset was implemented in the BATS model configuration. In these tests, RegCM3–BATS simulates the root zone soil moisture to be about 5–20% drier than in the RegCM3–BATS simulation, a difference slightly lower than in the original RegCM3–CLM3 simulation (about 15–30%). However with the revised soil texture, precipitation does not change more than 20% (results not shown). This suggests that these changes in soil moisture do not translate into the substantial precipitation change that is seen in the RegCM3–CLM3 simulation (Fig. 3). Thus, while the soil texture may be a trigger for the land–atmosphere coupling differences between the two models, the physical parameterizations in RegCM3–CLM3 allow those soil moisture changes to be communicated more effectively to the atmosphere.

4.1.2 Runoff and soil water storage

Within each region, the seasonal cycle of precipitation and soil moisture has a strong influence on the surface water budget components (including surface runoff, evapotranspiration, and storage of water in the soil). Therefore, we display the three components normalized to precipitation (Fig. 7). The fraction of precipitation contributing to runoff—or the runoff coefficient—is similar between the two models (Fig. 7; i.e., runoff/precipitation). On a per unit precipitation basis, RegCM3–CLM3 shows slightly higher runoff in the Guinean Coast region, and slightly less runoff in the Sahel. Runoff in the Northern Africa region is nearly identical between the two simulations.

The increased water input in the RegCM3–BATS simulation increases the soil water storage in all regions and all seasons (Table 2). Even when normalized to precipitation, RegCM3–BATS still tends to store more water in the soil than the RegCM3–CLM3, with the exception in the Guinean Coast region during the spring (advance) and fall (retreat) months due to an underestimate of precipitation during JJA. This greater storage in the RegCM3–BATS soil is likely due to the revised soil texture classification. In contrast, the sandier soils in RegCM3–CLM3 lead to greater infiltration and base flow runoff and reduced soil water storage.

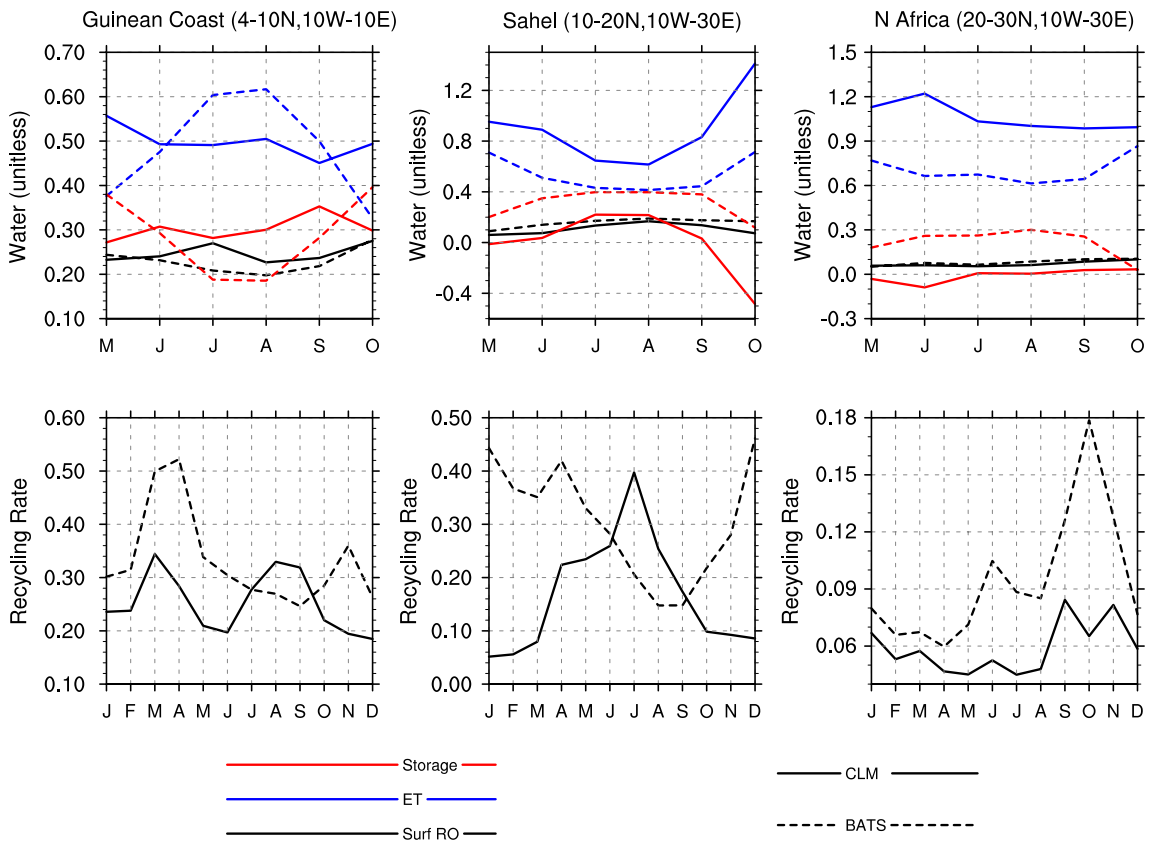

Fig. 7 Surface water balance. *Top panel*: Average seasonal normalized water balance terms, including evapotranspiration (*blue*), surface runoff (*black*), and calculated storage (*red*) for RegCM3–CLM3 (*solid lines*) and RegCM3–BATS (*dashed lines*) simulations for the three regions. Normalized components are divided by the total monthly incoming precipitation (*unitless*). Bottom panel: Precipitation recycling factor (β) as calculated from Eq. 1 for RegCM3–BATS (*black dashed line*) and RegCM3–CLM3 (*black solid line*)

Table 2 Summer season (JJA) surface energy and water balances

	Energy terms (W m^{-2})					Water terms (mm H_2O month^{-1})			
	SW In	SW Abs	Net LW	SH	LH	Precip	ET	Srf RO	Storage
Guinean Coast									
BATS	170.9	147.6	33.8	9.0	110.6	6.6	3.6	1.4	1.6
CLM	197.5	153.7	36.1	4.9	79.3	5.3	2.6	1.3	1.4
Sahel									
BATS	236.3	187.3	59.4	40.3	98.3	6.9	3.1	1.2	2.6
CLM	288.3	214.3	82.6	44.1	62.9	3.1	2.1	0.4	0.6
Northern Africa									
BATS	319.6	232.7	116.6	92.4	25.3	1.3	0.8	0.1	0.4
CLM	344.6	249.9	135.1	86.9	10.5	0.3	0.3	0.02	−0.02

4.1.3 Evapotranspiration and precipitation recycling

Total evapotranspiration (ET) is also substantially greater in the RegCM3–BATS simulation than in the RegCM3–CLM3 simulation (Table 2). However, the normalized ET (Fig. 7) shows that over most time periods and locations, RegCM3–CLM3 returns more water to the atmosphere via ET per unit precipitation than RegCM3–BATS. In the Sahel and Northern Africa regions, the RegCM3–CLM3 normalized ET is consistently greater than in RegCM3–BATS over the monsoon season. In the Guinean Coast region, the RegCM3–CLM3 produces more ET than RegCM3–BATS during the dry season. During the peak monsoon months, the normalized ET is enhanced in RegCM3–BATS due to the reduction in precipitation and cloud cover from the passage of the monsoon front. For most months and regions, however, the greater ET per unit precipitation in RegCM3–CLM3 returns more water to the atmosphere, thereby contributing to the drier soils in the RegCM3–CLM3 simulation.

An analysis of precipitation recycling (β; Eq. 1) over the regions further elucidates the relationship between the surface water balance and precipitation over the region (Fig. 7). The ET component of β varies seasonally following precipitation (Fig. 3), and is greater in RegCM-BATS in all regions and seasons. The difference in β between the two simulations is primarily due to a change in moisture advection. In RegCM-BATS, more moisture is advected into the Guinean Coast and Sahel regions along the western boundary during the monsoon season than in RegCM3–CLM3, which leads to lower β values in RegCM3–BATS during the monsoon season. In RegCM3–CLM3, the β peak in ASO is due to a greater contribution of ET, consistent with the increased contribution to the normalized ET shown in the top panel of Fig. 7. In the North Africa region, moisture advection is similar between the two simulations, yet total ET is greater in RegCM-BATS (Table 2), leading to an increased β value in this region. Overall, RegCM3–BATS has greater moisture advection along the western boundary during the monsoon season, resulting in lower recycling rates in the Guinean Coast and the Sahel. In contrast, RegCM3–CLM3 has a greater recycling rate during the monsoon season due to the increased importance of the ET component. The differences in moisture advection are described below in greater detail (Sect. 5).

4.2 Surface energy balance

4.2.1 Surface radiation balance

In all cases, incoming solar radiation is greater in RegCM3–CLM3 than in RegCM3–BATS (Fig. 8), due to reduced precipitation (Fig. 3) and cloud cover. This increase in the RegCM3–BATS precipitation leads to greater cloud liquid water content, increasing the amount of outgoing radiation (Fig. 9). This effect is particularly clear in the Sahel and Northern Africa regions, where the differences between the two simulations occur mainly during the wet season (March–October in the Sahel region, and April–September in the Northern Africa region). However, the increase in incoming solar radiation in RegCM3–CLM3 does not lead to the same increase in the amount of absorbed solar radiation (Fig. 8). This discrepancy suggests that the wetter soils in RegCM3–BATS lead to lower albedos and increased absorption of solar radiation (Fig. 8). This effect is known as the "soil-wetness feedback" or "enhanced albedo effect." Figure 10 shows the seasonal evolution of the surface albedo for the two simulations, with greater albedos in the RegCM3–CLM3 simulation south of 15°N. In the Guinean Coast region (4–10°N), RegCM3–BATS albedos are consistently lower than RegCM3–CLM3, where the soil tends to be saturated throughout the year and has a damped seasonal cycle. In the Sahel (10–20°N) and Northern Africa (20–30°N), the RegCM3–BATS albedos show a strong seasonal cycle that

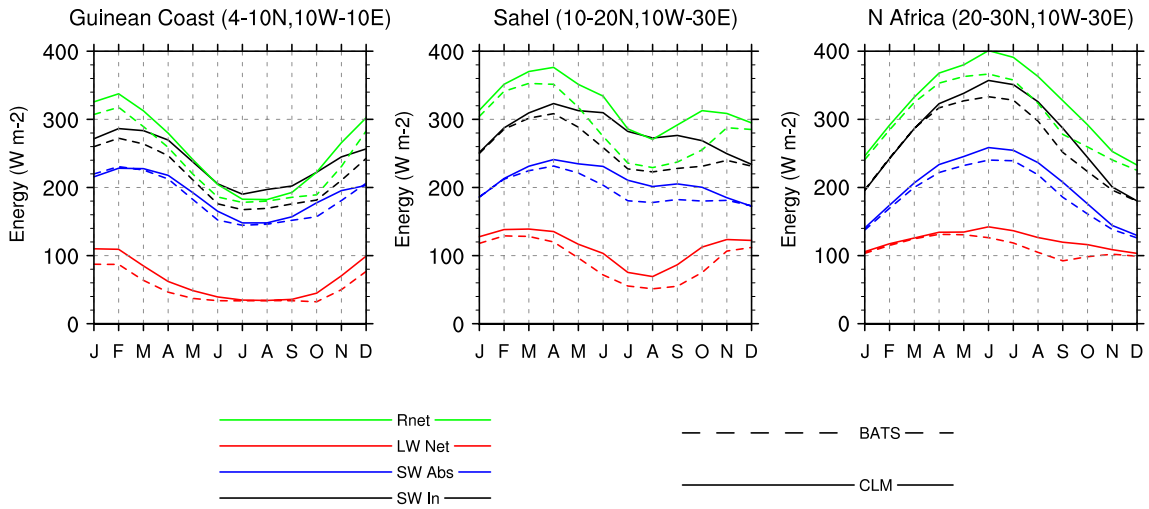

Fig. 8 Average seasonal surface radiation balance (terms in W m^{-2}) for the three African regions for RegCM3–CLM3 (*solid lines*) and RegCM3–BATS (*dashed lines*) simulations, including incoming shortwave radiation (*black*), absorbed shortwave (*blue*), net longwave (*red*), and total net radiation (*green*)

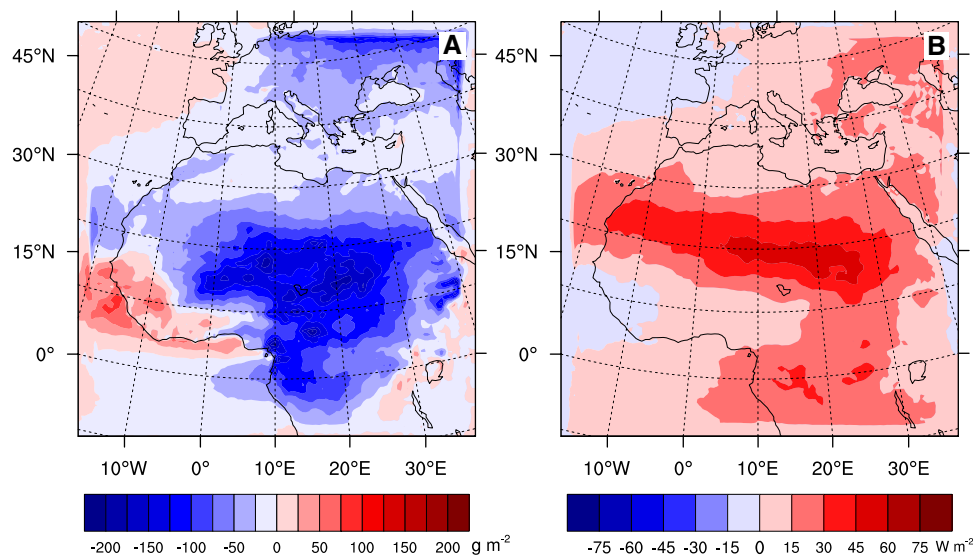

Fig. 9 Seasonal JJA average simulation difference (RegCM3–CLM3–RegCM3–BATS) of (**a**) the total column cloud liquid water content (g m^{-2}) and (**b**) outgoing longwave radiation at the top of the atmosphere (W m^{-2})

follows the soil moisture content. In contrast, the RegCM3–CLM3 simulation is less influenced by the seasonal cycle of soil moisture; the albedos change less than 0.04 over the course of the year.

RegCM3–BATS and RegCM3–CLM3 soil moisture–albedo relationships are parameterized in the same manner, where bare soil albedo is reduced by up to half of the dry soil value when precipitation occurs. Particularly in the Sahel and Guinean Coast regions, the RegCM3–BATS albedos are more sensitive to changes in soil wetness. This is likely creating a secondary feedback in RegCM3–BATS, where wetter soils further reduce the soil albedo, causing an enhanced feedback to absorbed solar radiation. This effect is particularly evident in the Guinean Coast region, although it is also noted in the Sahel and Northern Africa regions during the rainy season. The albedo effect's impact on the general circulation is discussed further in Sect. 5.

The net longwave radiation is also consistently greater in RegCM3–CLM3 than in RegCM3–BATS (Fig. 8). In general, the net longwave radiation budget is predominantly a balance between the changes in surface temperature and atmospheric moisture. An increase in the net longwave radiation (positive upwards) can be due to changes in downward longwave radiation (e.g., from atmospheric water vapor and clouds) or the amount of outgoing longwave radiation (e.g., from a change in surface temperature). In the Guinean Coast, net longwave radiation is typically greater in RegCM3–CLM3 than RegCM3–BATS, with the exception of the peak monsoon months when the values are similar. This is due to greater

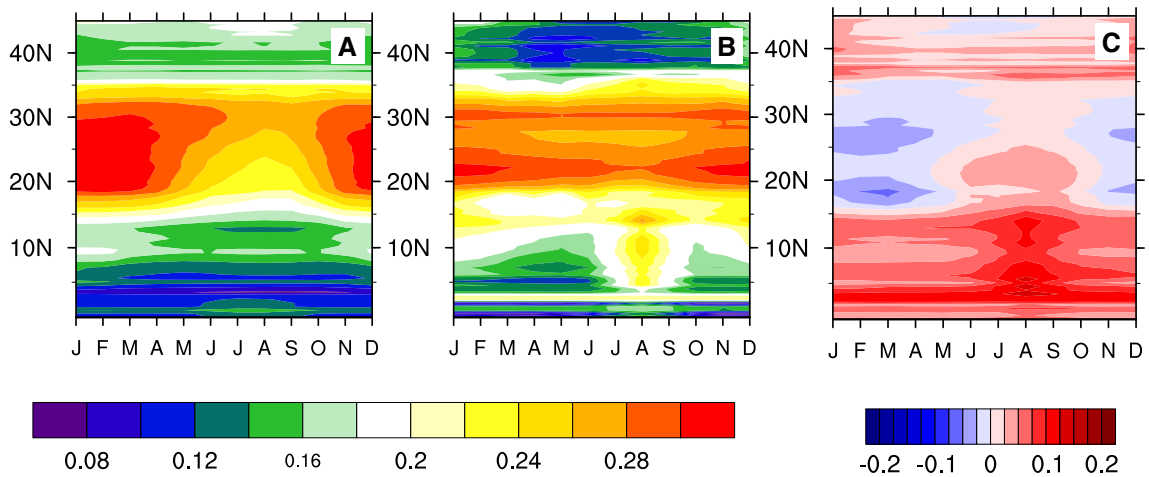

Fig. 10 Average seasonal meridional albedo (averaged from 10W to 10E and over the 10 year simulation period) for (**a**) RegCM3–BATS, (**b**) RegCM3–CLM3, and (**c**) the difference between these two simulations (CLM3–BATS)

downward longwave radiation in RegCM3–BATS ($\sim$10 W m^{-2}), and can be explained by the larger amount of cloud liquid water content in RegCM3–BATS (Fig. 9). In the Sahel and Northern Africa regions, the net longwave radiation in the RegCM3–CLM3 simulation is consistently greater than in RegCM3–BATS due to lower downward longwave radiation and greater outgoing longwave radiation.

Overall, the total net radiation (shortwave absorbed + net longwave) is greater in RegCM3–CLM3 over all regions in all seasons due to more absorbed shortwave radiation and greater net longwave radiation.

4.2.2 Sensible and latent heat fluxes

The sensible and latent heat fluxes are substantially different in the two simulations, with lower latent heat fluxes in RegCM3–CLM3 due to lower soil moisture and reduced total ET. These fluxes are compared with sensible and latent heat fluxes from the ALMIP experiment for representative dry and wet years (Fig. 11). In the Guinean Coast, RegCM3–CLM3 shows good agreement with the latent heat fluxes during the monsoon season, while RegCM3–BATS overestimates the latent heat flux due to increased precipitation. Both simulations underestimate the sensible heat fluxes in the Guinean Coast region, likely due to soils that are too wet and cool in the region (see discussion below). In the Sahel region, the latent heat fluxes from RegCM3–CLM3 show good agreement with the ALMIP fluxes, and an improved agreement of sensible heat flux. In contrast, the latent heat fluxes are too high in RegCM3–BATS.

This apparent overestimation of latent heat fluxes in RegCM3–BATS is important because higher latent heat fluxes increase the moist entropy flux and the amount of convective available potential energy in the boundary layer, likely increasing the frequency and magnitude of convective rainfall events (e.g., Pal and Eltahir 2001). Not surprisingly, the seasonal pattern of the latent heat flux differences between the two simulations matches that of precipitation and soil moisture. As a result of drier soils and reduced latent heating, sensible heat fluxes are generally higher in RegCM3–CLM3 than in the RegCM3–BATS simulation. One exception occurs during JAS in the Guinean Coast region, where the RegCM3–BATS simulation erroneously simulates a precipitation minimum when the monsoon front has incorrectly passed completely to the north. This precipitation minimum dries the RegCM3–BATS soils in July and August, leading to enhanced sensible heat fluxes.

4.2.3 Surface temperatures

Changes in the soil moisture and surface water and energy budgets impact surface temperatures (Fig. 12). In the tropical Guinean Coast region, monthly averaged temperatures vary only slightly during the year, ranging from 23°C to 29°C in the CRU observations. The RegCM3–BATS simulation is cooler than the CRU observations by 1–3°C over the course of the full seasonal cycle in the Guinean Coast region, likely due to relatively wet soils in RegCM3–BATS. The agreement between simulated and observed temperatures is improved in the RegCM3–CLM3 simulation during the dry season months (October through May). However, during the peak monsoon season (JJA), there is a negative temperature bias in both simulations likely due to an underestimate of sensible heat fluxes (Fig. 11).

Over the Sahel, drier soils in the RegCM3–CLM3 simulation are associated with a reduced cold bias

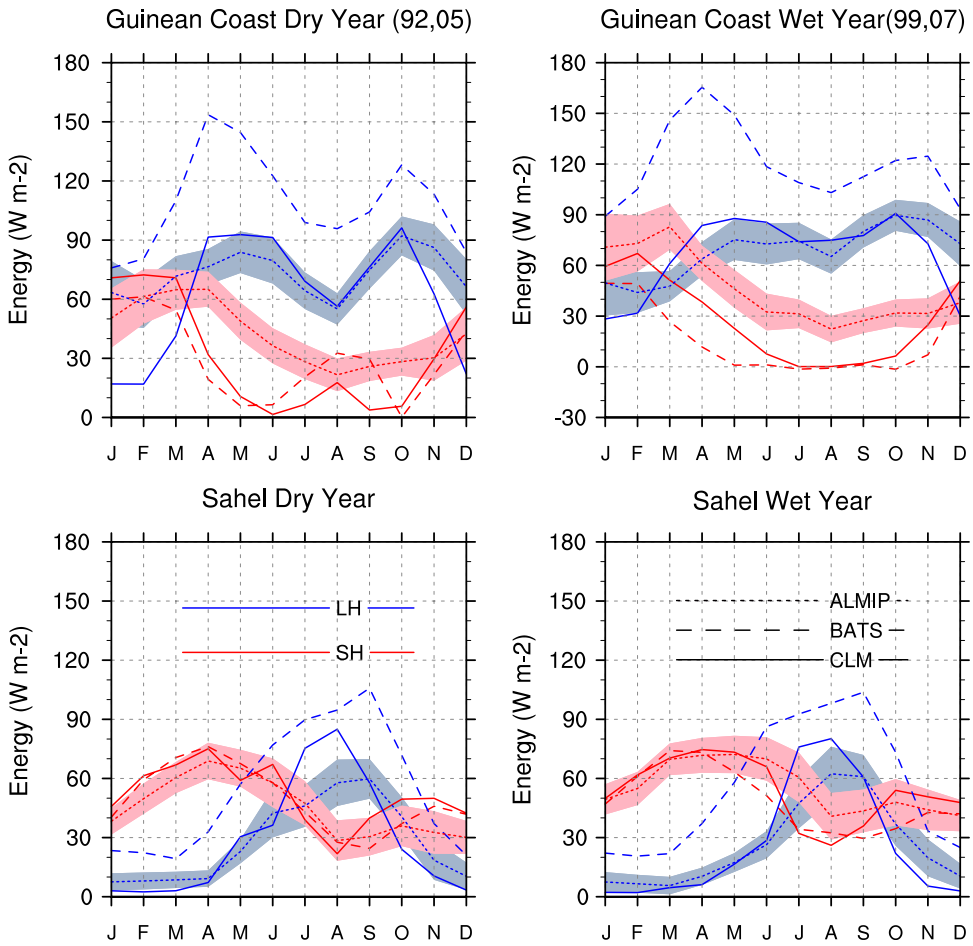

Fig. 11 Comparison of sensible (*red*) and latent (*blue*) heat flux terms (W m^{-2}) for the Guinean Coast and Sahel regions for a representative dry year (1992 for RegCM3–CLM3 (*solid line*) and RegCM3–BATS simulations (*dashed line*); 2005 for ALMIP (*dotted line*)) and a representative wet year (1999 for RegCM3–CLM3 and RegCM3–BATS simulations; 2007 for ALMIP). *Shaded regions* around the ALMIP fluxes indicate one standard deviation of the model spread

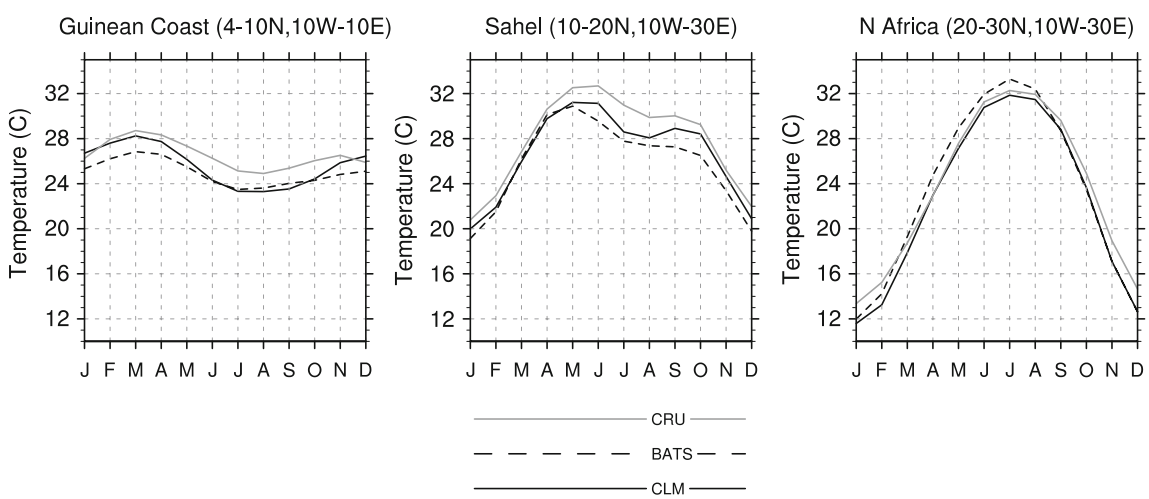

Fig. 12 Average seasonal 2 m surface temperature (°C) for the three West African regions (Guinean Coast, Sahel and Northern Africa) over the 10 year simulation period (1992–2001) for observations (CRU; Mitchell et al. 2004; *gray solid*), RegCM–CLM3 simulations (*black solid*), and RegCM3–BATS (*black dashed*) simulations

throughout the seasonal cycle. These drier surface soils lead to lower surface evaporation rates and latent heat fluxes, causing higher temperatures in RegCM3–CLM3 that are closer to observations. In the Northern Africa region, the RegCM3–BATS simulates a warm bias of about 1°C during the monsoon months (March–August) and a cold bias in the remainder of the year. RegCM3–CLM3 temperatures show a cold bias of up to 2°C in the dry

seasons months of October–February (less than that noted in CCSM-CLM3 simulations of Northern Africa, Dickinson et al. 2006), but an improved match to observations in the monsoon months.

Surface temperature can be important for the regional-scale circulation, as the meridional temperature and soil moisture gradients are known to contribute to the monsoon dynamics in western Africa (Emanuel 1995; Eltahir and Gong 1996; Sultan and Janicot 2003; Ramel et al. 2006). Figure 13 shows a meridional temperature cross section for the RegCM3–BATS and RegCM3–CLM3 simulations, respectively, averaged over longitudes from 10°W to 10°E. In both simulations, the seasonal migration of the temperature maximum moves from around 10°N in the spring to approximately 30°N in the wet season, and then moves south to approximately 10°N in SON. Because of drier soils and clearer skies, RegCM3–CLM3 is warmer in the monsoon band (5–20°N) over most of the seasonal cycle (Fig. 12). Additionally, the RegCM3–CLM3 simulation shows a temperature maximum dipole, with the first maximum occurring in May–June at 15–20°N, and a second maximum occurring in July at 25°N (Fig. 13b). This dipole is similar to that simulated by Ramel et al. (2006), and has been shown to control the position of the SHL and influence the inland progression of the monsoon. If the temperature maximum is located too far to the north, as in the RegCM3–BATS simulation, this could force the monsoon to travel further northwards.

Previously, the location of the temperature maximum has been strongly linked to the surface albedo (Sultan and Janicot 2003; Ramel et al. 2006). In our simulations, the surface albedo differs between the two simulations due to (1) changes in the soil classification (Sect. 2.3) and (2) changes in soil moisture (Sect. 4.1.2). As shown in Fig. 10 and discussed in Sect. 4.1.2, RegCM3–BATS has higher albedos throughout the Guinean Coast and Sahel regions, leading to less solar radiation absorbed and cooler temperatures. It is likely that the improvements in the surface temperature simulated by RegCM3–CLM3 are related to the improvement of the soil boundary conditions and their impact on soil moisture and albedo.

Triggered by changes in soil wetness and albedo, the surface meridional temperature gradient differs between the two simulations. Here we calculate the gradient using a centered finite difference algorithm. As a result of the temperature differences described above, the RegCM3–BATS simulation has a stronger surface temperature gradient than the RegCM3–CLM3 simulation (Fig. 14), with differences of up to 0.01°C/60 km beginning at the onset of the monsoon season (April) and continuing until September. The RegCM3–CLM3 temperature gradients are about half the values of the RegCM3–BATS gradients, peaking at 0.005°C/60 km. This meridional gradient is important for the formation and location of the African Easterly Jet and the northward penetration of the monsoon (see Sect. 5).

5 Impact of LSP on land surface–atmosphere interactions

As described above, the change in LSP causes a reduction in soil moisture in RegCM–CLM3, leading to a reduced amount of total evapotranspiration. In this section, we investigate how these land surface property changes propagate into the atmosphere via the MSE, causing a change in the monsoon circulation.

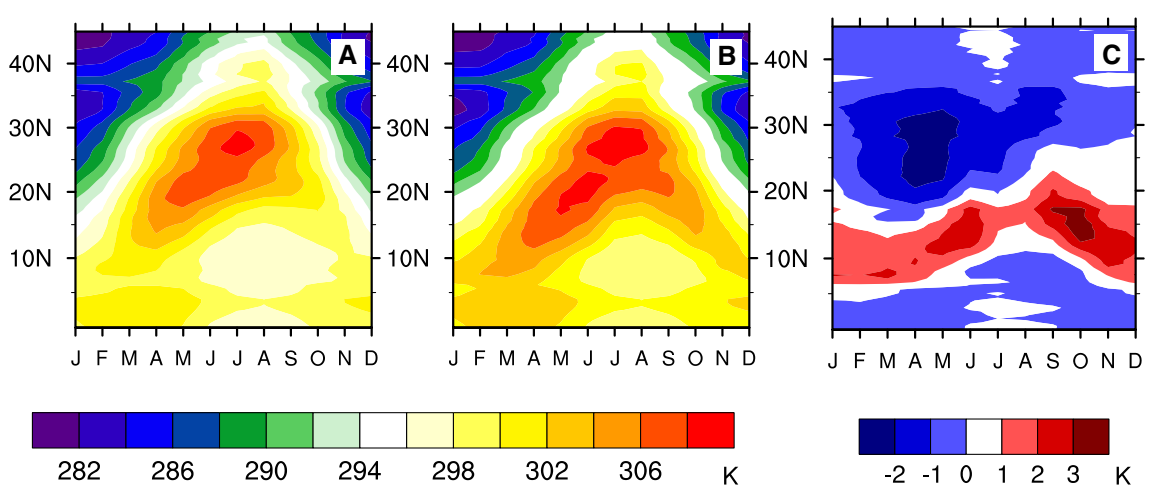

Fig. 13 Average seasonal meridional surface temperature (averaged from 10°W to 10°E and over the 10 year simulation period) for (**a**) RegCM3–BATS, (**b**) RegCM3–CLM3, and (**c**) the difference between these two simulations (CLM3–BATS)

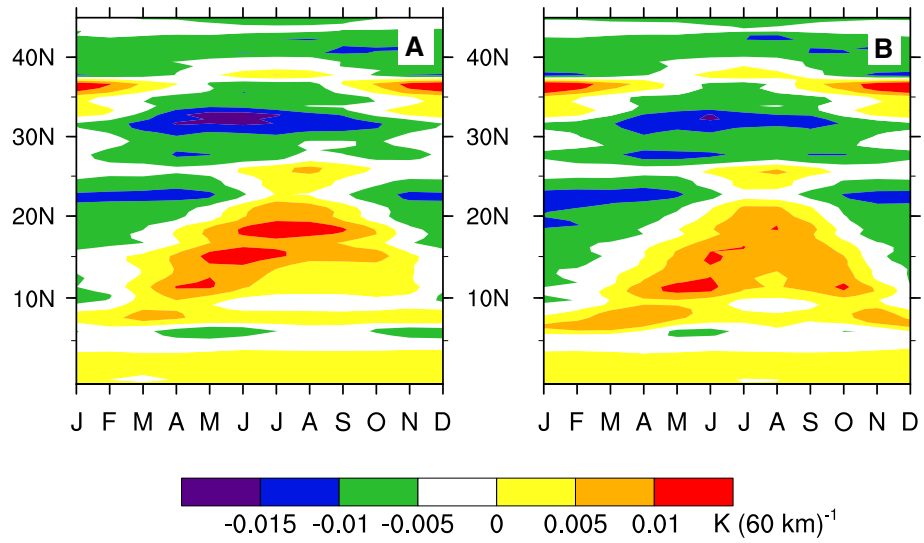

Fig. 14 Meridional surface temperature gradient (deg K (60 km)$^{-1}$) for (**a**) RegCM3–BATS simulations and (**b**) RegCM3–CLM3 simulations. Gradients are calculated using a centered finite difference scheme between model grid cells in the meridional direction

5.1 Moist static energy

Moist static energy (MSE) is an indicator of convection (Polcher 1995), with greater MSE leading to increased convection and precipitation. This increased precipitation can cause wetter soils and lower air temperatures at the surface, resulting in more precipitation. MSE values reach up to 350 kJ/kg over western Africa during the monsoon season (Fontaine et al. 2002), and the location of this maximum moves meridionally following the seasonal evolution of the monsoon (Fig. 15). Typically, MSE values tend to be higher during the monsoon onset than the monsoon retreat, leading to a seasonal asymmetry. In our simulations, the seasonal evolution of the zonally averaged surface MSE shows that the RegCM3–BATS MSE is greater than the RegCM3–CLM3 MSE over the monsoon belt throughout the full seasonal cycle (Fig. 15).

Three components contribute to MSE: the geopotential, sensible and latent energies (Eq. 2). Sensible energy provides the dominant component, followed by the geopotential energy (with increasing importance away from the surface), and small contributions from the latent energy (with decreasing importance away from the surface). Among these three components, the latent energy is the main contribution to the difference between RegCM-BATS and RegCM–CLM3 (Fig. 16). In JJA, wetter soils and increased moisture advection in RegCM-BATS north of 15°N lead to an increase in the release of water vapor to the atmosphere, increasing the amount of latent energy from the surface up to 300 hPa. South of 15°N, RegCM–CLM3 has a greater latent energy term due to the slower advance of the monsoon. Following the latent energy contribution, the sensible energy also contributes to the MSE due to drier and warmer conditions in RegCM–CLM3 near the surface.

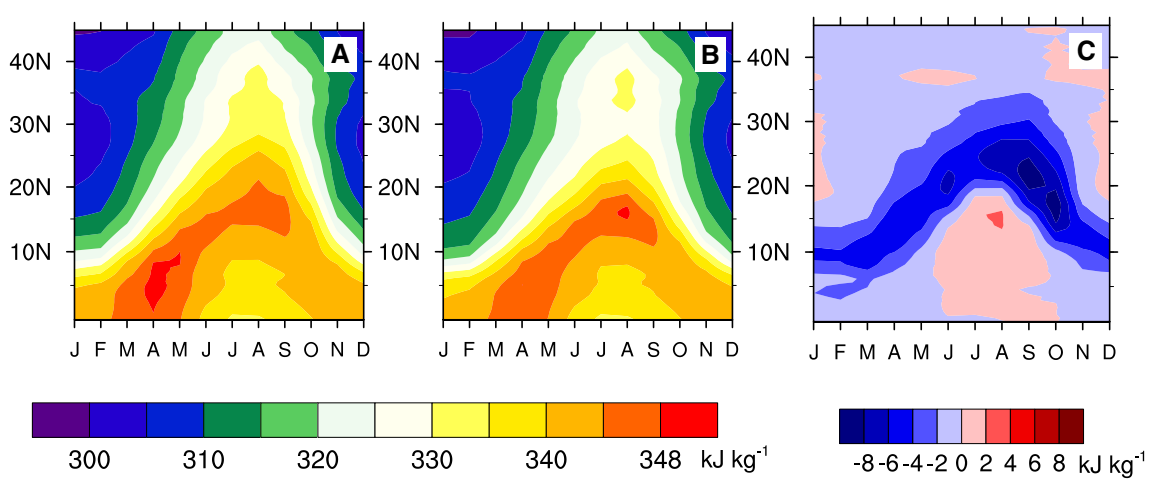

Fig. 15 Average seasonal meridional moist static energy (kJ kg^{-1}) (averaged from 10°W to 10°E and over the 10 year simulation period) for (**a**) RegCM3–BATS, (**b**) RegCM3–CLM3, and (**c**) the difference between these two simulations (CLM3–BATS)

In addition to the magnitude of MSE, the MSE gradient from the Guinean Coast to Northern Africa is known to influence the position and penetration of the monsoon from the Guinean coast into Northern Africa (Eltahir and Gong 1996). The gradient of MSE gives an indication of the location of baroclinic zones and the likelihood of potential energy generation, which can be converted to kinetic energy and drive the monsoon circulation (Emanuel 1995; Fontaine et al. 2002). Wet soil anomalies in the Guinean Coast region, particularly in the preceding winter, tend to lead to strong springtime surface MSE gradients (Philippon and Fontaine 2002). A strong MSE gradient yields deep convection and enhances the monsoon circulation, which is evident in the RegCM3–BATS experiments. The greater MSE in the RegCM3–BATS simulation tends to trigger more convection and precipitation, strengthening the monsoon and driving it further inland than in the RegCM3–CLM3 simulation.

5.2 Position of AEJ and large-scale circulation

To evaluate the AEJ, we first compare the JJA 600 hPa winds from the two RegCM3 simulations with the ERA40 reanalysis data (Fig. 17). In ERA40, the center of the Sahara high is located at approximately 30°N and 5°W, with strong westerlies to the north over Europe and easterlies to the south over southwestern Africa. The RegCM3–CLM3 circulation compares well with the ERA40 reanalysis, and reproduces the position of the Sahara high and the easterly outflow from the Guinean Coast region, although at a slightly weaker (2–3 m s^{-1}) strength. However, there are large differences between the RegCM3–BATS simulation and ERA40. In the RegCM3–BATS simulation, an anomalous cyclonic circulation is present over the Sahel region, centered at 10°N and between 0 and10°E.

Near the surface (850 hPa), the SHL is evident in both simulations at approximately 20°N and 0–10°W. In the RegCM3–BATS simulation, the SHL is much stronger than in the ERA40 reanalysis, and it is positioned at about 22°N (Fig. 17). In the RegCM3–CLM3 simulation, a weaker low is present at about 20°N; this position is in better agreement with ERA40. The strong SHL in RegCM3–BATS creates a strong westerly circulation from 8° to 15°N, which accounts for the increased inland moisture advection and reduced precipitation recycling noted in Sect. 4.1.3. In contrast, the RegCM3–CLM3 850 hPa winds indicate less moisture influx from the western

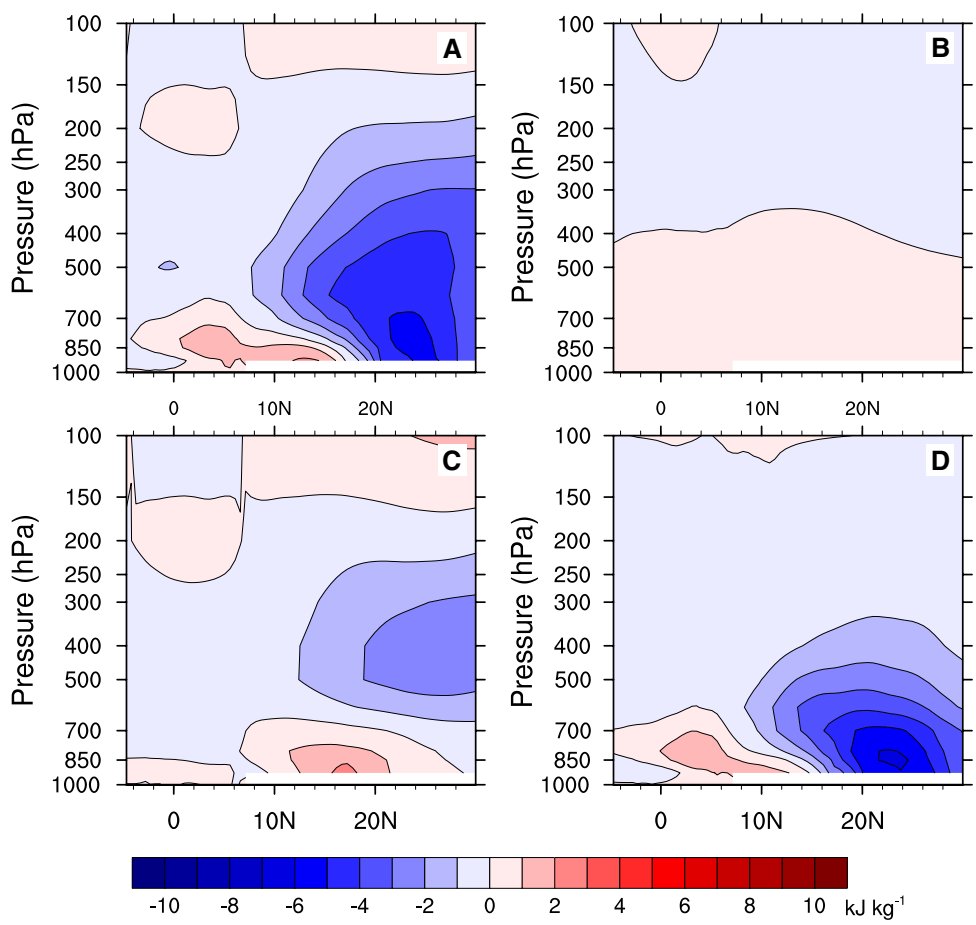

Fig. 16 Difference in the MSE and MSE components between the RegCM3–CLM3 and RegCM3–BATS simulations (spatially averaged from 10°W to 10°E during JJA) as a function of latitude and pressure levels for (**a**) total MSE, (**b**) the geopotential contribution to MSE, (**c**) the sensible energy contribution to MSE, and (**d**) the latent energy contribution to MSE. Units in kJ kg^{-1}

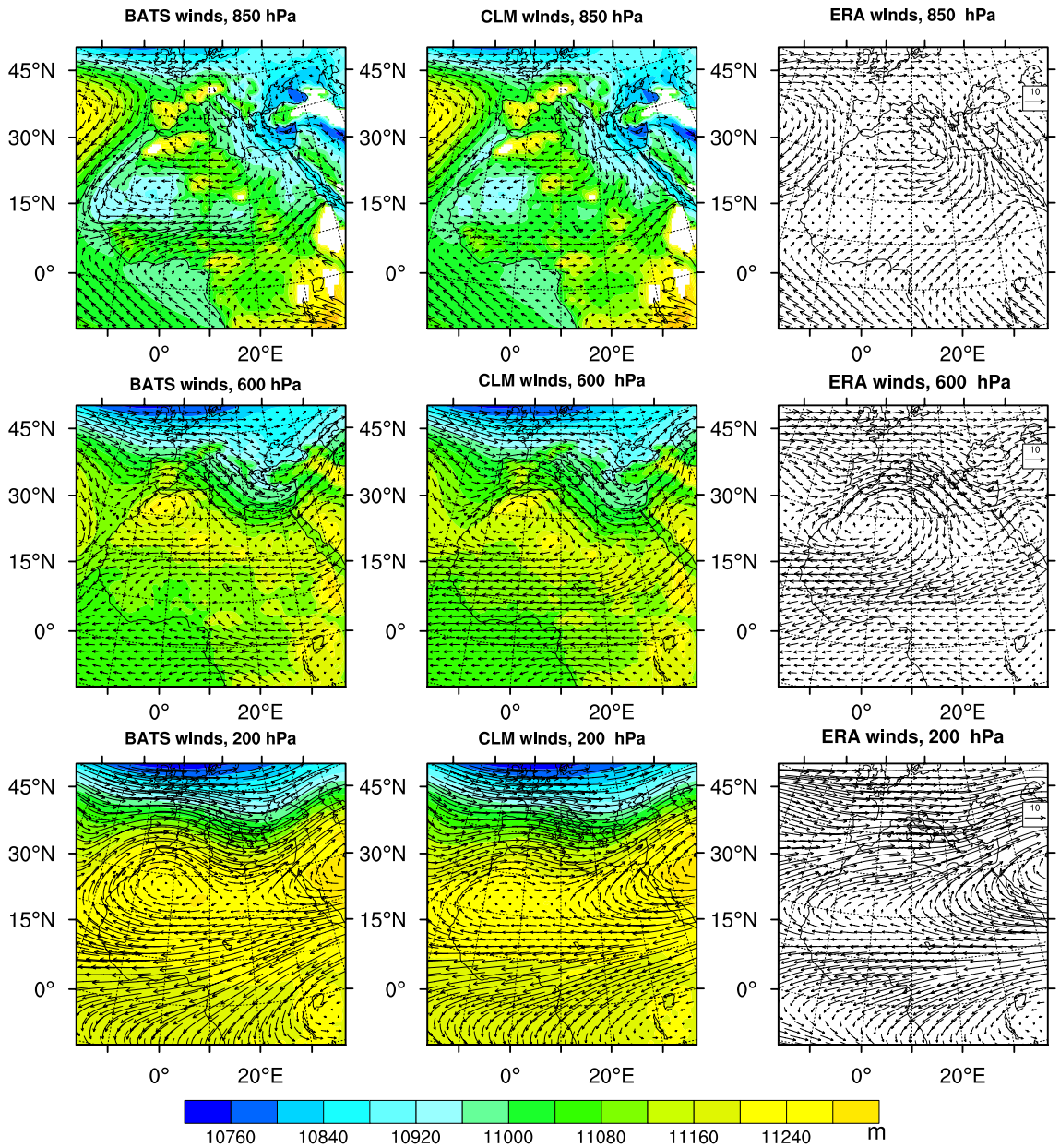

Fig. 17 Mean JJA wind vectors for RegCM3–BATS simulations, RegCM3–CLM3 simulations, and the driving ERA-40 Reanalysis data at the 850 hPa, 600 hPa and 200 hPa vertical heights. Geopotential heights for the model simulations are shown in color contours (m)

boundary, accounting for greater precipitation recycling in RegCM3–CLM3.

As with other circulation features, there are substantial differences in the simulation of the AEJ in the two RegCM3 simulations. The latitudinal position of the AEJ depends upon the location of the strongest surface temperature gradient via the thermal wind balance (e.g., Burpee 1972; Cook 1999; Thorncroft and Blackburn 1999; Sultan and Janicot 2003; Thorncroft et al. 2003), and is found at the height where the positive meridional temperature gradient becomes negative in the mid-troposphere at ~600 hPa. The surface temperature gradient relationship is seen in the simulated position of the jet (Fig. 18) relative to the simulated surface temperature gradient (Fig. 14). The surface temperature gradient is stronger and displaced northward in RegCM3–BATS simulation compared to RegCM3–CLM3. In May, the RegCM3–BATS surface temperature gradient maximum is at about 12°N, with the strongest portion of the AEJ at ~15°N. In June, the surface temperature gradient peaks at 15°N, with the AEJ maximum at 18°N. In July, the surface temperature gradient moves to ~18°N and the position of the AEJ peaks at 19°N. However, in August, the AEJ disappears in the RegCM3–BATS simulation. Throughout the monsoon

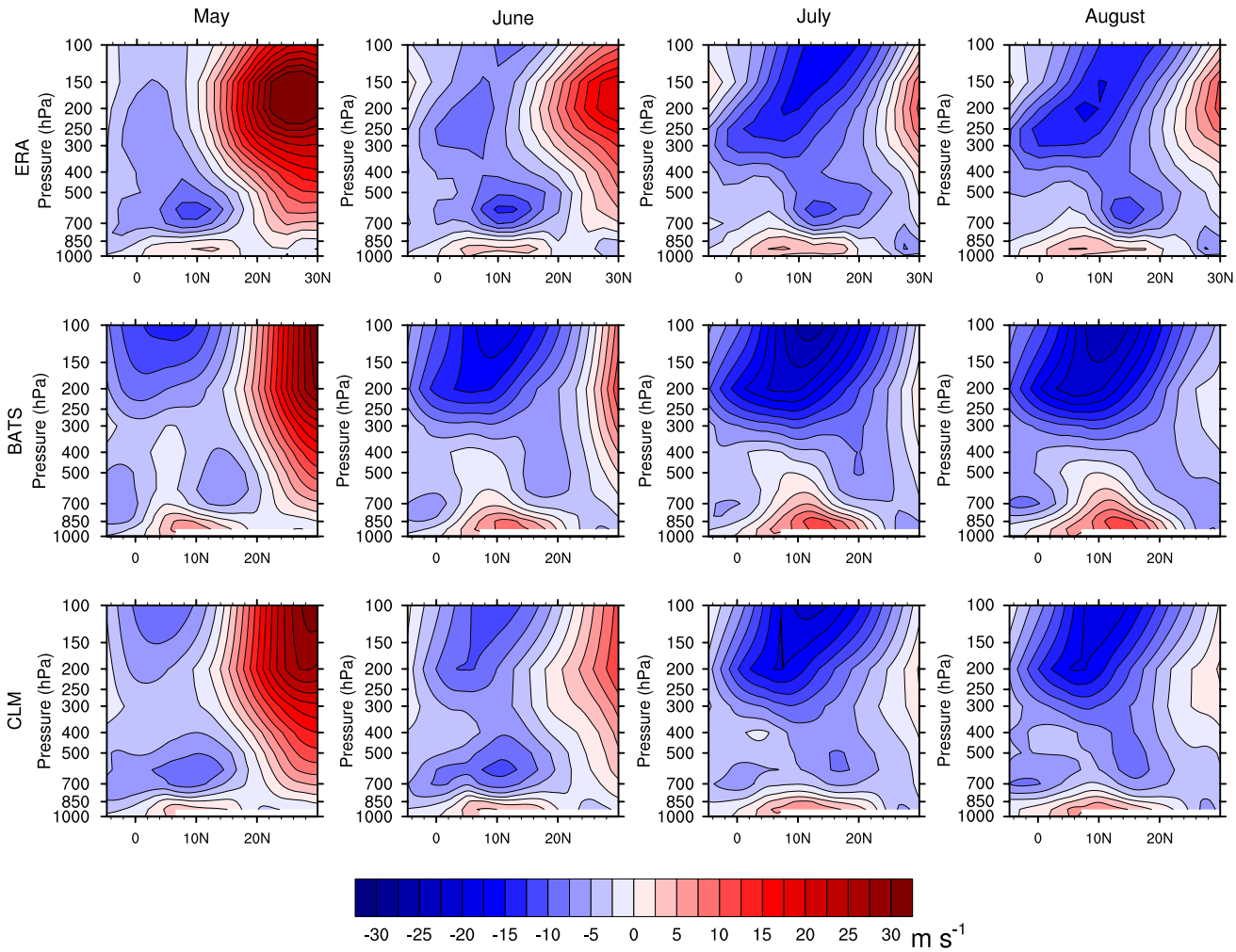

Fig. 18 Monthly averaged zonal winds (m s^{-1}) (spatially averaged from 10°W to 10°E) as a function of latitude and pressure levels for the ERA-40 Reanalysis (Uppala et al. 2005), RegCM3–BATS, and RegCM3–CLM3. The African Easterly Jet is located at approximately 650 hPa at 0–20°N, depending upon the month

season, the RegCM3–BATS AEJ is weak and located too far northward compared to the ERA40 driving fields.

The weakening and disappearance of the AEJ in the RegCM3–BATS simulation appear to be associated with the strengthening of the SHL between 20 and 30°N (Fig. 17 at 850 hPa). The SHL increases in height from May to August (Fig. 18), reaching up to 500 hPa in the RegCM3–BATS simulation. The northward penetration of the monsoon front likely changes the SHL from a dry, shallow thermal low to a deeper, moister system (Peyrillé and Lafore 2007; Patricola and Cook 2008). The moist equatorial westerlies extend into the midtroposphere, which is characteristic of wet years in the Sahel (Grist and Nicholson 2001). This increase in moisture at higher altitudes can be seen via the Lq term of MSE in Fig. 16d. In addition, the Saharan High is weakened compared to the ERA40 driving fields (Fig. 17; 600 hPa). The net result of these changes is that RegCM3–BATS maintains a positive meridional temperature gradient throughout the troposphere as shown in Fig. 19, and the AEJ is weakened or absent throughout the monsoon season. In contrast, RegCM3–CLM3 has a reversal in sign of the meridional temperature gradient at ~600 hPa, and the strength of the jet is maintained at 5–10 m s^{-1} throughout the monsoon season (Fig. 18). At upper levels, the Tropical Easterly Jet (TEJ) is stronger in RegCM3–BATS (Fig. 17) as a result of this positive temperature gradient throughout the troposphere.

These RegCM3–BATS results are consistent with observational studies that find a weaker, northward-displaced AEJ and stronger TEJ when rainfall is above average over the Sahel (Newell and Kidson 1984; Grist and Nicholson 2001). In addition, model sensitivity studies show similar dynamical changes when soil moisture is increased over the Sahel, or when grassland is replaced with forest (e.g., Xue and Shukla 1996; Patricola and Cook 2008). Indeed, in the RegCM3–CLM3

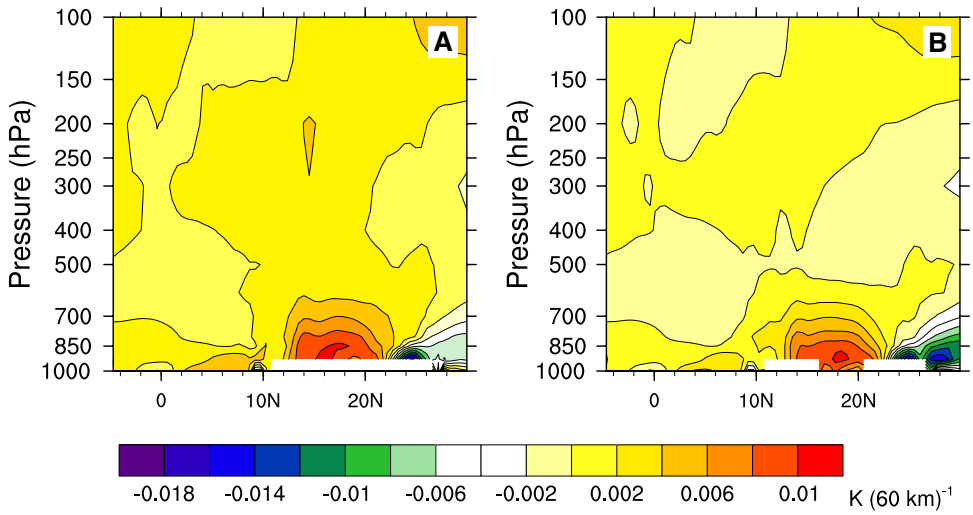

Fig. 19 Mean JJA vertical meridional temperature gradients, averaged at 15°W (as in Patricola and Cook 2008) for (**a**) RegCM3–BATS simulations and (**b**) RegCM3–CLM3 simulations. Units are in degrees K (60 km)$^{-1}$

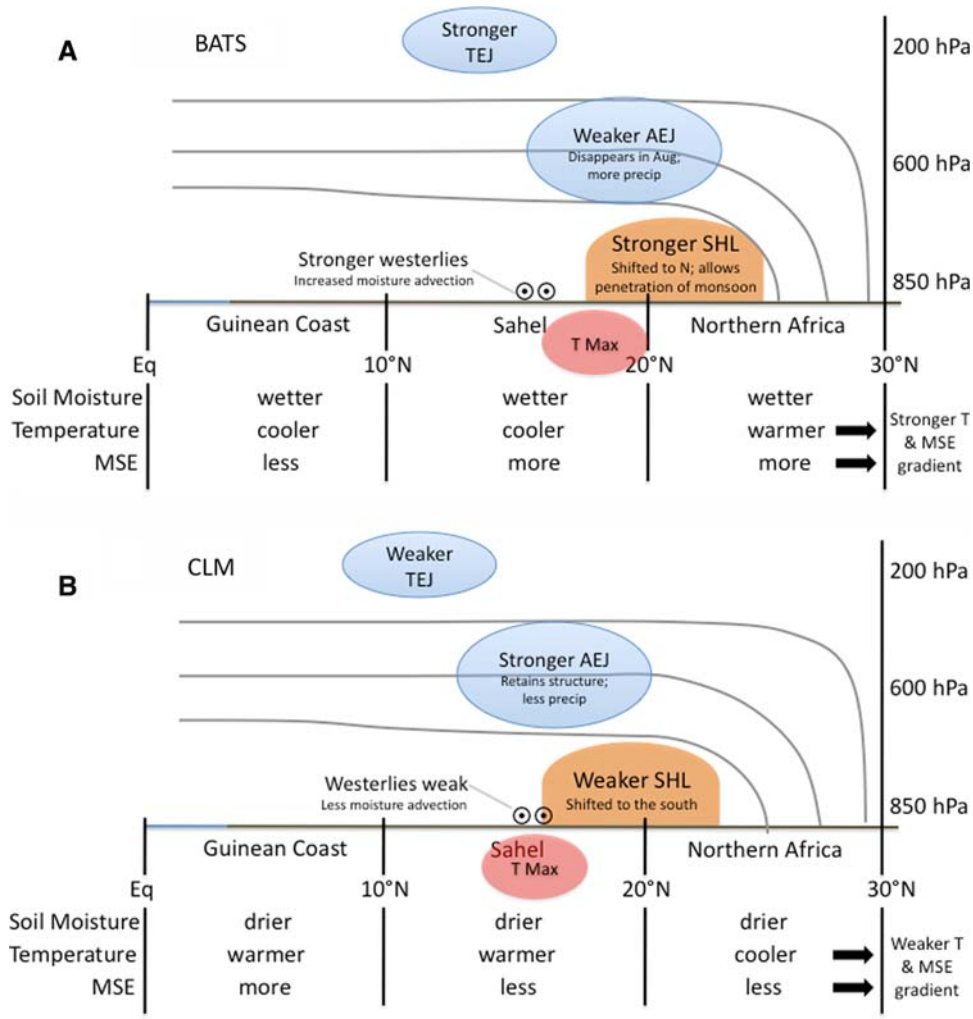

Fig. 20 Schematic representation of the JJA atmospheric dynamics over West Africa for the two RegCM3 simulations. Land surface and dynamical features are described as a relative comparison between (**a**) RegCM3–BATS simulation and (**b**) RegCM3–CLM3 simulation. *Gray lines* indicate adiabats

simulation, the monsoon does not penetrate as far northward, and the position, magnitude, and temporal evolution of the AEJ and the SHL more closely match the ERA40 reanalysis (Fig. 18). This result appears to confirm again that land surface properties have an important effect on the location and strength of the AEJ.

6 Discussion and conclusion

We have compared two simulations of regional climate over West Africa, focusing on the impact of the LSP on the regional monsoon circulation. The difference in land surface model physics greatly affects the simulation of the West African monsoon precipitation, leading to a substantial improvement in performance for the RegCM3–CLM3 model configuration. The precipitation difference between the RegCM3–CLM3 and RegCM3–BATS simulations is triggered by changes in the physical description of the land surface, which yields drier soils and increased evapotranspiration per unit precipitation in the RegCM3–CLM3.

The mechanism of these land–atmosphere interactions is summarized in Fig. 20. In RegCM3–BATS, wetter soils lead to a stronger meridional surface temperature and MSE gradient (Fig. 20a). The excess surface heating in RegCM3–BATS deepens the SHL, inducing an anomalous circulation around 10°N in JJA, bringing additional moisture in from the west and into the lower troposphere, thereby weakening the AEJ. The changes in the latitudinal profiles of temperature and MSE over the span of the monsoon season lead to a weakening and northward shift of the AEJ. Comparatively, the drier RegCM3–CLM3 simulation has weaker temperature and MSE gradients that lead to a more southerly position of the jet (Fig. 20b). The RegCM3–CLM3 simulation does not produce this erroneous circulation, and as a result the 600 hPa winds are qualitatively similar to the ERA40 reanalysis winds and show continued outflow of air over the Guinean coast.

One key difference between the two LSPs is the soil texture boundary condition, with a more detailed distribution of the sand and clay content in the RegCM3–CLM3 configuration. Additionally, these differences in soil texture combined with the hydrologic treatment of the soil column lead to greater infiltration, less water storage in the soil, and drier soils in western and northern Africa in the RegCM3–CLM3. Differences are also evident between the evapotranspiration components of the water cycle. RegCM3–CLM3 returns less total water to the atmosphere than BATS, yet more per unit precipitation, thereby increasing the precipitation recycling during the monsoon season. The net result is drier soils in RegCM3–CLM3 that trigger strong land surface–atmosphere feedbacks involving the monsoon circulation and precipitation. This improvement reinforces the concept that changes in land surface conditions can cause substantial changes in the atmospheric circulation over West Africa. From our decadal-scale simulations, it is impossible to separate the influence of the soil texture boundary condition from the influence of the hydrologic treatment of the soil column. However, our additional sensitivity studies indicate that the soil texture may be a trigger for the land–atmosphere coupling differences between the two models, with the physical parameterizations in RegCM3–CLM3 allowing those soil moisture changes to propagate more effectively into the atmosphere.

Prior studies have shown that the land surface is an important component in simulations of the West African monsoon and the regional climate dynamics. The results presented here indicate that regional monsoon precipitation is highly sensitive to the selection of LSP and land surface boundary conditions. Changes in these boundary conditions can in fact propagate throughout the atmosphere to affect the simulation of dynamical features such as the SHL and AEJ. This sensitivity highlights the importance of the land surface processes in accurately forecasting regional precipitation, particularly in regions of land–atmosphere hotspots such as West Africa.

Acknowledgments This work was supported in part by NSF awards 0315677 and 0450221 to LCS and NSD. We gratefully acknowledge the European Centre for Medium-Range Weather Forecasts for the use of the ERA-40 data. We also acknowledge the use of CMAP Precipitation data provided by the NOAA/OAR/ESRL PSD, Boulder, Colorado, USA (http://www.cdc.noaa.gov/), and the contributed simulations of the ALMIP Working Group: G. Balsamo, P. de Rosnay, A. Beljaars, C. Delire, P. Harris, C. Taylor, T. Orgeval, J. Polcher, A. Ducharne, A. Nørgaard, I. Sandholt, Y. Xue, I. Poccard-Leclercq, S. Gascoin, Y. Gusev, O. Nasonova, S. Saux-Picart, C. Ottle, and B. Decharme. We thank Benjamin Lintner and Adrian Tompkins for useful discussions.

References

Abiodun BJ, Pal JS, Afiesimama EA, Gutowski WJ, Adedoyin A (2008) Simulation of the West African monsoon using RegCM3, Part II: impacts of deforestation and desertification. Theor Appl Climatol 93:245–261. doi:10.1007/s00704-007-0333-1

Afiesimama EA, Pal JS, Abiodun BJ, Gutowski WJ Jr, Adedoyin A (2006) Simulation of West African monsoon using the RegCM3. Part I: model validation and interannual variability. Theor Appl Climatol 86:23–37. doi:10.1007/s00704-005-0202-8

Betts AK, Ball JH (1995) The FIFE surface diurnal cycle climate. J Geophys Res 100:25679–25693. doi:10.1029/94JD03121

Betts AK, Ball JH, Beljaars ACM, Miller MJ, Viterbo PA (1996) The land-surface interaction: a review based on observational and global modeling perspectives. J Geophys Res 101:7209–7225. doi:10.1029/95JD02135

Bonan GB, Levis S, Kergoat L, Oleson KW (2002) Landscape as patches of plant functional types: an integrating concept for climate and ecosystem models. Global Biogeochem Cycles 16:2. doi:10.1029/2000GB001360

Boone A, deRosnay P (2007) Towards the improved understanding of land-surface processes and coupling with the atmosphere over West Africa. iLEAPS Newl 3:33–34

Burpee RW (1972) The origin and structure of easterly waves in the lower troposphere. J Atmos Sci 29:77–90. doi:10.1175/1520-0469(1972)029<0077:TOASOE>2.0.CO;2

Charney JG, Quirk WJ, Chow S, Kornfield J (1977) A comparative study of the effects of albedo change on droughts in semi-arid regions. J Atmos Sci 34:1366–1385. doi:10.1175/1520-0469(1977)034<1366:ACSOTE>2.0.CO;2

Chou C, Neelin JD (2003) Mechanisms limiting the northward extent of the northern summer convection zones. J Clim 16:406–425. doi:10.1175/1520-0442(2003)016<0406:MLTNEO>2.0.CO;2

Cook KH (1999) Generation of the African Easterly Jet and its role in determining West African precipitation. J Clim 12:1165–1184. doi:10.1175/1520-0442(1999)012<1165:GOTAEJ>2.0.CO;2

Cook KH, Vizy EK (2006) Coupled model simulations of the West African Monsoon System: twentieth and twenty-first-century simulations. J Clim 19(15):3681–3703. doi:10.1175/JCLI3814.1

Cosgrove BA et al (2003) Land surface model spin-up behavior in the North American Land Data Assimilation System (NLDAS). J Geophys Res 108(22):8845. doi:10.1029/2002JD003316

Dai Y-J et al (2003) The common land model. Bull Am Meteorol Soc 84(8):1013–1023. doi:10.1175/BAMS-84-8-1013

de Goncalves LGG, Shuttleworth WJ, Burke EJ, Houser P, Toll DL, Rodell M, Arsenault K (2006) Toward a South America Land Data Assimilation System: aspects of land surface model spin-up using the simplified simple biosphere. J Geophys Res 111: D17110. doi:10.1029/2005JD006297

Dickinson R, Henderson-Sellers A, Kennedy P (1993) Biosphere-atmosphere transfer scheme (BATS) version 1e as coupled to the NCAR community climate model. Technical report, National Center for Atmospheric Research

Dickinson RE et al (2006) The community land model and its climate statistics as a component of the community climate system mode. J Clim 19:2302–2324. doi:10.1175/JCLI3742.1

Diedhiou A, Mahfouf J-F (1996) Comparative influence of land and sea surfaces on the Sahelian drought: a numerical study. Ann Geophys 14:115–130. doi:10.1007/s00585-996-0115-6

Dirmeyer PA, Gao X, Zhao M, Guo Z, Oki T, Hanasaki N (2006) GSWP-2: multi-model analysis and implications for our perception of the land surface. Bull Am Meteorol Soc 87:1381–1397. doi:10.1175/BAMS-87-10-1381

Douville H, Conil S, Tyteca S, Voldoire A (2007) Soil moisture memory and West African monsoon predictability: artefact or reality? Clim Dyn 28(7–8):723–742. doi:10.1007/s00382-006-0207-8

Eltahir EAB, Gong C (1996) Dynamics of wet and dry years in West Africa. J Clim 9(5):1030–1042. doi:10.1175/1520-0442(1996)009<1030:DOWADY>2.0.CO;2

Emanuel KA (1991) A scheme for representing cumulus convection in large-scale models. Q J R Meteorol Soc 48:2313–2335

Emanuel KA (1995) On thermally direct circulations in moist atmosphere. J Atmos Sci 52(9):1529–1533. doi:10.1175/1520-0469(1995)052<1529:OTDCIM>2.0.CO;2

FAO/UNESCO (1974) Soil Map of the World. Volume I: legend. UNESCO, Paris, France

Fontaine, B, Philippon N, Trzaska S, Roucou P (2002) Spring to summer changes in the West African monsoon through NCEP/NCAR reanalyses (1968–1998). J Geophys Res 107:D14, 4186. doi:10.1029/2001JD000834

Fontaine B, Louvet S, Roucou P (2007) Fluctuations in annual cycles and interseasonal memory in West Africa: rainfall, soil moisture and heat fluxes. Theor Appl Climatol 88:57–70. doi:10.1007/s00704-006-0246-4

Gallée H et al (2004) A high-resolution simulation of a West African rainy season using a regional climate model. J Geophys Res D05108. doi:10.1029/2003JD004020

Giannini A, Saravanan R, Chang P (2003) Oceanic forcing of Sahel rainfall on interannual to interdecadal time scales. Science 302:1029–1030. doi:10.1126/science.1089357

Giorgi F, Bates G (1989) The climatologic al skill of a regional model over complex terrain. Mon Weather Rev 117:2325–2347. doi:10.1175/1520-0493(1989)117<2325:TCSOAR>2.0.CO;2

Giorgi F, Bates G, Nieman S (1993) The multi-year surface climatology of a regional atmospheric model over the western United States. J Clim 6:75–95. doi:10.1175/1520-0442(1993)006<0075:TMSCOA>2.0.CO;2

Giorgi F, Pal JS, Bi X, Sloan L, Elguindi N, Solmon F (2006) Introduction to the TAC special issue: the RegCNET network. Theor Appl Climatol 86:1–4. doi:10.1007/s00704-005-0199-z

Global Soil Data Task (2000) Global Soil Data Products CD-ROM (IGBP-DIS). CD-ROM. International Geosphere-Biosphere Programme, Data and Information System, Potsdam, Germany. Available from Oak Ridge National Laboratory Distributed Active Archive Center, Oak Ridge, Tennessee, U.S.A. [http://www.daac.ornl.gov]

Grell GA (1993) Prognostic evaluation of assumptions used by cumulus parameterizations. Mon Weather Rev 121(3):764–787. doi:10.1175/1520-0493(1993)121<0764:PEOAUB>2.0.CO;2

Grell GA, Dudhia J, Stauffer D (1994) A description of the fifth-generation Penn State/NCAR mesoscale model (MM5). Technical report NCAR/TN-398 + STR, National Center for Atmospheric Research

Grist JP, Nicholson SE (2001) A study of the dynamic factors influencing the rainfall variability in the West African Sahel. J Clim 14:1337–1359. doi:10.1175/1520-0442(2001)014<1337:ASOTDF>2.0.CO;2

Holtslag A, de Bruijn E, Pan H-L (1990) A high resolution air mass transformation model for short-range weather forecasting. Mon Weather Rev 118:1561–1575. doi:10.1175/1520-0493(1990)118<1561:AHRAMT>2.0.CO;2

Janicot S, Trzaska S, Poccard I (2001) Summer Sahel-ENSO teleconnection and decadal time scale SST variation. Clim Dyn 18:303–320. doi:10.1007/s003820100172

Joly M et al (2007) African monsoon teleconnections with tropical SSTs: validation and evolution in a set of IPCC4 simulations. Clim Dyn 29:1–20. doi:10.1007/s00382-006-0215-8

Kiehl J, Hack J, Bonan G, Boville B, Breigleb B, Williamson D, Rasch P (1996) Description of the NCAR community climate model (CCM3). Technical report NCAR/TN-420 + STR, National Center for Atmospheric Research

Konaré, A, Zakey A, Solmon F, Giorgi F, Rauscher S, Ibrah SS, Bi X (2008) A regional climate modeling study of the effect of desert dust on the West African monsoon. J Geophys Res 113:D12, D12206. doi:10.1029/2007JD009322

Koster RD, Suarez MJ (1992) A comparative analysis of two land surface heterogeneity representations. J Clim 5(12):1379–1390. doi:10.1175/1520-0442(1992)005<1379:ACAOTL>2.0.CO;2

Koster RD, Suarez MJ (2003) Impact of land surface initialization on seasonal precipitation and temperature prediction. J Hydrometeorol 4:408–423. doi:10.1175/1525-7541(2003)4<408:IOLSIO>2.0.CO;2

Koster RD et al (2003) Observational evidence that soil moisture variations affect precipitation. Geophys Res Lett 30(5):1241. doi:10.1029/2002GL016571

Koster RD et al (2004) Regions of strong coupling between soil moisture and precipitation. Science 305:1138–1140. doi:10.1126/science.1100217

Loveland TR et al (2000) Development of a global land cover characteristics database and IGBP DISCover from 1-km AVHRR data. Int J Remote Sens 21:1303–1330. doi:10.1080/014311600210191

Meehl GA et al (2006) Monsoon regimes in the CCSM3. J Clim 19(11):2482–2495. doi:10.1175/JCLI3745.1

Messager C, Gallee H, Brasseur O (2004) Precipitation sensitivity to regional SST in a regional climate simulation during the West African monsoon for two dry years. Clim Dyn 22:249–266. doi:10.1007/s00382-003-0381-x

Mitchell TD, Carter TR, Jones PD, Hulme M, New M (2004) A comprehensive set of high-resolution grids of monthly climate

for Europe and the globe: the observed record (1901–2000) and 16 scenarios (2001–2100). Working paper, Tyndall Centre

Newell RE, Kidson JW (1984) African mean wind changes between Sahelian wet and dry periods. J Climatol 4:1–7. doi:10.1002/joc.3370040102

Oleson KW et al (2004) Technical description of the Community Land Model. NCAR technical note NCAR/TN-461 + STR, 186 pp

Paeth H, Friederichs P (2004) Seasonality and time scales in the relationship between global SST and African rainfall. Clim Dyn 23:815–837. doi:10.1007/s00382-004-0466-1

Pal J, Eltahir EAB (2001) Pathways relating soil moisture conditions to future summer rainfall within a model of the land-atmosphere system. J Clim 14(6):1227–1242. doi:10.1175/1520-0442(2001)014<1227:PRSMCT>2.0.CO;2

Pal JS, Eltahir EAB (2003) A feedback mechanism between soil moisture distribution and storm tracks. Q J R Meteorol Soc 129(592):2279–2297. doi:10.1256/qj.01.201

Pal JS, Small EE, Eltahir EAB (2000) Simulation of regional-scale water and energy budgets: representation of subgrid cloud and precipitation processes within RegCM. J Geophys Res 105(D24):29579–29594. doi:10.1029/2000JD900415

Pal JS et al (2007) Regional climate modeling for the developing world: the ICTP RegCM3 and RegCNET. Bull Am Meteorol Soc 88(9):1395–1409. doi:10.1175/BAMS-88-9-1395

Parker DJ, Thorncraft CD, Burton RR, Diongue-Niang A (2005) Analysis of the African easterly jet, using aircraft observations from the JET2000 experiment. Q J R Meteorol Soc 131:1461–1482. doi:10.1256/qj.03.189

Patricola CM, Cook KH (2008) Atmosphere/vegetation feedbacks: a mechanism for abrupt climate change over northern Africa. J Clim 113:D18102. doi:10.1029/2007JD009608

Peyrillé P, Lafore J-P (2007) An idealized two-dimensional framework to study the West African monsoon. Part II: large-scale advection and the diurnal cycle. J Atmos Sci 64:2783–2803. doi:10.1175/JAS4052.1

Philippon N, Fontaine B (2002) The relationship between the Sahelian and previous 2nd Guinean rainy seasons: a monsoon regulation by soil wetness? Ann Geophys 20:575–582

Polcher J (1995) Sensitivity of tropical convection to land surface processes. J Atmos Sci 52(17):3143–3163. doi:10.1175/1520-0469(1995)052<3143:SOTCTL>2.0.CO;2

Ramel R, Gallee H, Messager C (2006) On the northward shift of the West African monsoon. Clim Dyn 26:429–440. doi:10.1007/s00382-005-0093-5

Reynolds RW, Rayner NA, Smith TM, Stokes DC, Wang W (2002) An improved in situ and satellite SST analysis for climate. J Clim 15:1609–1625. doi:10.1175/1520-0442(2002)015<1609:AIISAS>2.0.CO;2

Rowell DP (2001) Teleconnections between the tropical Pacific and the Sahel. Q J R Meteorol Soc 127:1683–1706. doi:10.1002/qj.49712757512

Schär C, Luethi D, Beyerle U, Heise E (1999) Soil-precipitation feedback: a process study with a regional climate model. J Clim 12(3):722–741. doi:10.1175/1520-0442(1999)012<0722:TSPFAP>2.0.CO;2

Sellers PJ et al (1997) Modeling the exchanges of energy, water, and carbon between continents and the atmosphere. Science 275:502–509. doi:10.1126/science.275.5299.502

Sijikumar S, Roucou P, Fontaine B (2006) Monsoon onset over Sudan-Sahel: simulation by the regional scale model MM5. Geophys Res Lett 33:L03814. doi:10.1029/2005GL024819

Steiner AL, Pal JS, Giorgi F, Dickinson RE, Chameides WL (2005) Coupling of the Common Land Model (CLM0) to a regional climate model (RegCM). Theor Appl Climatol 82(3–4):225–243. doi:10.1007/s00704-005-0132-5

Sultan B, Janicot S (2003) The West African Monsoon dynamics. Part II: the preonset and onset of the summer monsoon. J Clim 16:3407–4327. doi:10.1175/1520-0442(2003)016<3407:TWAMDP>2.0.CO;2

Taylor CM, Parker DJ, Lloyd CR, Thorncroft CD (2005) Observations of synoptic-scale land surface variability and its coupling with the atmosphere. Q J R Meteorol Soc 131:913–937. doi:10.1256/qj.04.119

Thorncroft CD, Blackburn M (1999) Maintenance of the African easterly jet. Q J R Meteorol Soc 125:763–786. doi:10.1002/qj.49712555502

Thorncroft CD, Parker DJ, Burton RR, Diop M, Ayers JH, Barjat H, Devereau S, Diongue A, Dumelow R, Kindred DR, Price NM, Saloum M, Tayor CM, Tompkins AM (2003) The JET2000 Project: aircraft observations of the African Easterly Jet and African Easterly Waves. Bull Am Meteorol Soc 84(3):337–351. doi:10.1175/BAMS-84-3-337

Uppala SM et al (2005) The ERA-40 re-analysis. Q J R Meteorol Soc 131:2961–3012. doi:10.1256/qj.04.176

Vinnikov KY, Robok A, Speranskaya NA, Schlosser AC (1996) Scales of temporal and spatial variability of midlatitude soil moisture. J Geophys Res 101(3):7163–7174. doi:10.1029/95JD02753

Vizy EK, Cook KH (2001) Mechanisms by which Gulf of Guinea and Eastern North Atlantic sea surface temperature anomalies can influence African rainfall. J Clim 14:795–821. doi:10.1175/1520-0442(2001)014<0795:MBWGOG>2.0.CO;2

Wang G, Eltahir EAB (2000) The role of vegetation dynamics in enhancing the low-frequency variability of the Sahel rainfall. Water Resour Res 36(4):1013–1021. doi:10.1029/1999WR900361

Wilson MF (1984) The construction and use of land surface information in a general circulation climate model. Unpublished Ph.D. thesis, University of Liverpool, UK, 346 pp

Xie P, Arkin PA (1997) Global precipitation: a 17-year monthly analysis based on gauge observations, satellite estimates, and numerical model outputs. Bull Am Meteorol Soc 78:2539–2558. doi:10.1175/1520-0477(1997)078<2539:GPAYMA>2.0.CO;2

Xue Y, Shukla J (1996) The influence of land surface properties on Sahel climate. Part II: afforestation. J Clim 9:3260–3275. doi:10.1175/1520-0442(1996)009<3260:TIOLSP>2.0.CO;2

Zheng X, Eltahir EAB (1998) The role of vegetation in the dynamics of the west African monsoon. J Clim 11:2078–2096. doi:10.1175/1520-0442(1998)011<2078:TROVIT>2.0.CO;2